UNIVERSIDADE FEDERAL DE PERNAMBUCO

DEPARTAMENTO DE ENGENHARIA DE PRODUÇÃO

PROGRAMA DE PÓS-GRADUAÇÃO EM ENGENHARIA DE PRODUÇÃO

DEVELOPMENT OF A MULTI-OBJECTIVE GENETIC ALGORITHM TO REDUCE INDIVIDUAL RISK AND TRAVELLING TIME DURING EVACUATION IN TOXIC CLOUD RELEASE SCENARIOS

DISSERTATION PRESENTED TO UFPE

FOR THE MASTER'S DEGREE ATTAINMENT

BY

ERIKA OLIVEIRA DA SILVA

ADVISOR: MÁRCIO JOSÉ DAS CHAGAS MOURA, DSc.

RECIFE/2017

ERIKA OLIVEIRA DA SILVA

DEVELOPMENT OF A MULTI-OBJECTIVE GENETIC ALGORITHM TO REDUCE INDIVIDUAL RISK AND TRAVELLING TIME DURING EVACUATION IN TOXIC CLOUD RELEASE SCENARIOS

Master dissertation presented to UFPE for the master's degree attainment as part of the requirements of the Programa de Pós-Graduação em Engenharia de Produção (Concentration Area: Operations Research).

Advisor: Márcio José Das Chagas Moura, DSc

RECIFE/2017

Catalogação na fonte
Bibliotecária: Rosineide Mesquita Gonçalves Luz / CRB4-1361 (BCTG)

S586d Silva, Erika Oliveira da.
Development of a multi-objective genetic algorithm to reduce individual risk and travelling time during evacuation in toxic cloud release scenarios /Erika Oliveira da Silva. – Recife, 2017.
73f.: il., fig. tab.

Orientador: Prof. Dr. Márcio José Das Chagas Moura.

Dissertação (Mestrado) – Universidade Federal de Pernambuco. CTG. Programa de Pós-graduação em Engenharia de Produção, 2017.
Inclui Referências e Apêndices.

1. Engenharia de Produção. 2. Evacuation route. 3. Multi-objective optimization. 4. Genetic algorithm. 5. Evacuation time. 6. Individual risk. I. Moura, Márcio José Das Chagas (Orientador). II. Título.

658.5 CDD (22.ed) UFPE/BCTG-2018- 42

UNIVERSIDADE FEDERAL DE PERNAMBUCO
PROGRAMA DE PÓS-GRADUAÇÃO EM ENGENHARIA DE PRODUÇÃO

PARECER DA COMISSÃO EXAMINADORA PARECER DA COMISSÃO EXAMINADORA PARECER DA COMISSÃO EXAMINADORAPARECER DA COMISSÃO EXAMINADORADA COMISSÃO EXAMINADORA

DE DEFESA DE DISSERTAÇÃO DE MESTRADO DE

ERIKA OLIVEIRA DA SILVA

"DEVELOPMENT OF A MULTI-OBJECTIVE GENETIC ALGORITHM TO REDUCE INDIVIDUAL RISK AND TRAVELLING TIME DURING EVACUATION IN TOXIC CLOUD RELEASE SCENARIOS"

ÁREA DE CONCENTRAÇÃO: PESQUISA OPERACIONAL

A comissão examinadora composta pelos professores abaixo, sob a presidência do primeiro, considera o candidato **ERIKA OLIVEIRA DA SILVA**, **APROVADO.**

Recife, 19 de dezembro de 2017.

_____
Prof. MÁRCIO JOSÉ DAS CHAGAS MOURA, PhD (UFPE)

_____
Prof. ADIEL TEXEIRA DE ALMEIDA FILHO, PhD (UFPE)

_____
Prof. MARCELO RAMOS MARTINS, PhD (USP)

ACKNOWLEGDMENTS

Primeiramente gostaria de agradecer meus pais, Erick Francisco e Maria Luiza, por todo apoio para minha formação, tanto financeiramente como emocionalmente. Sem eles com certeza não teria alcançado metade do que alcancei profissionalmente.

A meu irmão e grande amigo, Erick Oliveira, que apesar da distância, sempre tem estado presente me apoiando e orientando. Agradeço também por ter me ajudado com sua experiência em linguagem C++ que utilizei no algoritmo desse trabalho.

À equipe CEERMA, em especial à Gisele de Lima, Caio Souto Maior, Rafael Azevedo, July Bias por ajudar e compartilhar o conhecimento e pelas discussões durante o desenvolvimento e principalmente na parte final desse trabalho. Agradeço também à Cláudia Cavalcanti e Joelma Maria pelos momentos de descontração durante os almoços e confraternizações.

A Paulo Estevão por sempre estar presente desde que nos conhecemos nos últimos anos da minha graduação, pela orientação, conselhos e apoio.

Ao PPGEP pelos novos conhecimentos adquiridos e estrutura disponibilizada.

Ao meu orientador Márcio Moura pela confiança depositada e ajuda durante a pesquisa e outras atividades que realizamos juntos.

À professora Isis Lins, por ter me ajudado com o tema de algoritmos genéticos, pela paciência e pela atenção em todos os momentos que precisei.

Aos meus antigos e novos amigos, em especial à Flávia Miranda, Thais Lima, Sara Lima e família que me proporcionaram muitos momentos de alegria e descontração durante a realização desse trabalho.

Ao CNPQ pelo suporte financeiro.

ABSTRACT

The evacuation route planning is one of the protective actions that can be implemented in cases of hazardous substance leakage. Some toxic releases accidents that occurred recently in Brazil, such as in port of Santos, and release of a toxic gas in Cubatão, highlights the importance of an evacuation planning. Evacuation is the most complex mitigation measure so detailed analysis must be performed before planning. That is the reason the present work proposes a multi-objective optimization problem to give more information for the decision maker. The MOP aims to minimize both evacuation time and individual risk during evacuation due to a H_2S release in some of the treatment units in a hypothetical oil refinery. First, the possible accidental scenarios, causes and consequences are identified. After that, the scenarios with toxic cloud release and high severity are selected to be simulated in ALOHA® software in order to calculate the toxic concentration in each node of the evacuation route. The previous information is used in a multi-objective genetic algorithm written in C++ that results in a set of non-dominated solutions. Each solution was studied and the routes that both considered a good compromise between time and individual risk were selected.

Keywords: Evacuation route. Multi-objective optimization. Genetic algorithm. Evacuation time. Individual risk.

RESUMO

O planejamento de rotas de evacuação é uma das ações de proteção que podem ser implementadas em casos de vazamento de substâncias perigosas. Alguns tóxicos liberados em acidentes ocorridos recentemente no Brasil, como no porto de Santos, e em Cubatão, destacam a importância de um planejamento de evacuação. A evacuação é a medida de mitigação mais complexa, e por essa razão uma análise detalhada deve ser realizada para ajudar no planejamento. Essa é a razão pela qual o presente trabalho propõe um problema de otimização multi-objetivo para dar mais informações ao tomador de decisão. O MOP visa minimizar o tempo de evacuação e o risco individual durante a evacuação devido a uma liberação de H_2S em algumas unidades de tratamento em uma refinaria de petróleo hipotética. Em primeiro lugar, são identificados os possíveis cenários acidentais, causas e consequências. Depois disso, os cenários com liberação de nuvem tóxica de alta severidade são selecionados para serem simulados no software ALOHA® e obter a concentração tóxica em cada nó da rota de evacuação. A informação anterior é utilizada em um algoritmo genético multi-objetivo escrito em C ++ que fornece como resultado um conjunto de soluções não-dominadas. Cada solução foi estudada e as rotas que consideraram um bom compromisso entre o tempo e o risco individual foram selecionadas.

Palavras-chave: Rotas de evacuação. Otimização multiobjetivo. Algoritmo Genético. Tempo de evacuação. Risco individual.

LIST OF ILLUSTRATIONS

LIST OF TABLES

LIST OF ABBREVIATIONS

ABIQUIM - Associação Brasileira da Indústria Química

AEGLs - Exposure Guideline Levels

APELL - Awareness and Preparedness for Emergency at Local Level

CAER - Community Awareness and Emergency Response

DFS – Depth First Search

GA - Genetic Algorithm

LOC – Level of Concern

MOGA - Multi objective Genetic Algorithm

MOP - Multi-Objective Problem

ERP - Emergency Response Planning

ILO - International Labour Organization

UN - United Nations

PHA - Preliminary Hazard Analysis

WSA - Wet Gas Sulfuric Acid

SUMMARY

1 INTRODUCTION

1.1 Opening Remarks

Many countries have been experienced major accidents in chemical and petrochemical industry that caused death of thousands of people and great environmental impacts in the surroundings. Among them, it could be mentioned Flixborough in England in 1974, Seveso in Italy in 1976 (ALE; KLUIN; KOOPMANS, 2017), Bhopal in India in 1984 (VUORIO; STOOP; JOHNSON, 2017), Mexico City in 1984 (ECKHOFF, 2014) and Sandoz in Switzerland in 1986 (MAHON; KELLEY, 1987). Many consequences of these disasters had long-term effects to the environment and population because consequences were aggravated due to lack of preparation and emergency plans (CETESB, 2017).

Huge accidental events are really uncommon and the decision-making process should consider all the uncertainties involved in the episodes (APOSTOLAKIS, 1989; GEORGIADOU et al., 2007; MILAZZO; AVEN, 2012). Risk analysis, identification and quantification are the fundamental step in the process of creating the Emergency Response Planning (ERP) to reduce risks. ERP is formed by diverse information in order to provide fast and effective actions in cases of emergency such as shelter for the population, evacuation procedures of the affected area and etc. (GEORGIADOU et al., 2007).

According to Li et al. (2010), making evacuation plans is a multi-objective problem in the context of operational research. There is an interest in simultaneously reducing two or more objectives, for example: reducing the risk of death of the people involved, costs, distance traveled and / or journey time. Some of these goals can be conflicting, such as minimizing risk and minimizing distance or travel time. A route that would be conducted in less time and distance may offer greater risk of fatality.

In this context, the multi-objective optimization problem (MOP) can be defined as the problem of finding a vector of decision variables that satisfies the constraints and optimizes the objective functions, which are frequently in conflict with each other though. Consequently, in MOP, the term “optimize” means to find a solution, where the values of the objective functions are interesting for the decision maker. Then, the term Pareto optimum is used (COELLO COELLO; LAMONT; VAN VELDHUIZEN, 2007). If the vector of decision variables $\boldsymbol{x}$ is Pareto optimal, there is no other feasible decision variables vector that can decrease (increase)

some criterion without causing a simultaneous increase (decrease) in at least one other criterion. This concept will hardly result in only a single solution, but in a set of solutions called Pareto optimal set. The vectors of the decision variables that correspond to the solutions of this set are called non-dominated. The objective functions plot, where the non-dominated vectors are in the Pareto optimal set, is called the Pareto frontier (COELLO COELLO; LAMONT; VAN VELDHUIZEN, 2007).

The wide use of genetic algorithms (GA) to solve multi-objective problems is justified by the possibility of calculating a set of solutions in only one run (GOERIGK; DEGHDAK; HESSLE, 2014). The ability of GA to search simultaneously in different regions of the solution space makes it possible to find a diverse set of solutions for difficult problems with nonconvex, discontinuous and multimodal spaces. Moreover, its crossover operator can reach different unknown parts of the Pareto front, finding new non-dominated solutions (KONAK; COIT; SMITH, 2006).

For this reason, the following dissertation aims to solve a multi-objective optimization problem, considering the total time of escaping as well as the risk of an individual along the path in accidental scenarios with toxic cloud release. The toxic substance considered was hydrogen sulfide, a highly toxic contaminant present in petroleum, which is discarded during the refining process. Accidental scenarios were simulated in some refinery treating units, where hydrogen sulfide streams can be easily found. The concentration values from the simulation were used to calculate the individual risk, and the multi-objective problem is solved by using a genetic algorithm.

1.2 Justification

The requirement of an effective response to an accidental release of chemicals has become a concern of governments after great accidents such as Bhopal in India. The accident in Bhopal highlighted the importance that the population near an industrial facility should be aware about the risks involved in the industrial activity and must be prepared for any accidental scenarios that may occur by monitoring the plant performance regarding to safety and environment (GUPTA, 2004).

Programs for risk mitigation have been promoted by the UN, ILO and business entities in Brazil (ABIQUIM) and worldwide such as: Emergency Planning and Community Right-to-

Know Act; CAER – Community Awareness and Emergency Response; APELL – Awareness and Preparedness for Emergency at Local Level, among others (MORAES, 2013).

Recent accidents in Brazil, such as the release of toxic gas from a container in the port of Santos (JORNAL ESTADÃO DIGITAL, 2017), and an explosion in a conveyor belt and tank, releasing a toxic gas from the combustion of ammonium nitrate in Cubatão (OLIVEIRA, 2017; VALE, 2017) emphasizes the importance of studies of analysis and optimization of escape routes for toxic cloud releases.

1.3 Objectives

1.3.1 General Objective

To solve the evacuation route optimization problem for each of the simulated toxic cloud events for oil refinery processing units using multi-objective genetic algorithm (MOGA).

1.3.2 Specific Objectives

- To identify main potential hazardous events that may cause toxic clouds;
- To formulate an MOP to minimize the evacuation time and individual risk for workers in the refinery;
- To implement MOGA to solve the MOP;
- To validate the MOGA solution found with the exhaustive method.
- To analyze the results from MOGA and choose the best evacuation routes, considering the best compromise between total time and the individual risk.

2 THEORETICAL BACKGROUND

2.1 Hazards and Contaminants Removal in Oil Refinery

2.1.1 Petroleum Composition and Contaminants

Petroleum is a complex mixture of organic chemicals that usually contains thousands of different compounds. These compounds are hydrocarbons, which contain only hydrogen and carbon, and hydrocarbons combined with a varying number of elements such as sulfur, nitrogen, oxygen and a small amount of metals such as nickel, vanadium, and chromium. The petroleum composition affects the oil properties and characteristics. The oil properties determine how the oil behaves in the environment (FINGAS, 2015).

Sulfur compounds are commonly found in crude oils and its content can vary considerably; see Table 2-1. These compounds are an undesirable contaminant because they are fetid, corrosive, and they poison the metallic catalysts used in the refining process. Most products have a standard limit on the amount of sulfur, and thus the refinery must remove the excess. Hence, the presence of sulfur compounds lowers the price of the petroleum. Nitrogen compounds are also an undesirable contaminant, because they poison the cracking catalysts and contribute to gum formation in final products (JAMES G. SPEIGHT, 1982). Therefore, both sulfur and nitrogen must be removed during the refining process.

Table 2-1: Crude oils typical composition (FINGAS, 2015) .

Elemental compound	**Composition (%)**
Carbon	83-87
Hydrogen	10-14
Sulfur	0.05-6
Nitrogen	0.1-2
Oxygen	0.05-1.5

The hydrotreating is a chemical process, where oil fractions are reacted with hydrogen at high temperature and high pressure in presence of a catalyst. The reaction saturates olefins or converts aromatics to naphthene and removes heteroatoms, Table 2-2. The sulfur and nitrogen

compounds are converted to hydrogen sulfide (H_2S) and ammonia (NH_3), respectively (Table 2-3), producing acid gas and sour gas.

Table 2-2: Oil fractions hydrotreated. Adapted from (FAHIM, M. A.; AL-SAHHAF, T. A.; ELKILANI, 2012).

Stream	**Products**	**Contaminant removed**
Naphtha	Reformer feed	Sulfur
Atmospheric gas oil	Diesel	Sulfur, aromatic compounds
Vacuum gas oil	Low Sulphur fuel oil (LSFO)	Sulfur
	FCC feed	Sulfur, nitrogen, metals
	Diesel	Sulfur, aromatic compounds
	Kerosene/Jet fuel	Sulfur, aromatic compounds
	Naphtha	Sulfur, aromatic compounds
	Lube oil	Sulfur, nitrogen, aromatic compounds
Residuum	LSFO	Sulfur
	FCC feedstock	Sulfur, nitrogen, aromatic compounds
	Coker feedstock	Sulfur, metals

Hydrogen sulfide is a colorless, highly toxic, flammable gas with a characteristic foul odor of rotten eggs. It is slightly denser than air, actually 1.18 times heavier. As a result, hydrogen sulfide accumulates easily in confined spaces (vessels, tanks, valve pits, drains) (FAHIM, M. A.; AL-SAHHAF, T. A.; ELKILANI, 2012). The inhalation of a low concentration of hydrogen sulfide (15-75 mg/m^3) can cause a great irritation in the respiratory tract and eyes, and the inhalation of a high concentration (150-432 mg/m^3) causes paralysis of olfactory nerve and chemical pneumonitis and a concentration higher than 864 mg/m^3 is fatal (XU; FAN, 2014).

Table 2-3: Some hydrotreating reactions.

Desulphurization	$RSH + H_2 \rightarrow RH + H_2S$
	$R_2S + 2H_2 \rightarrow 2RH + H_2S$
	$(RS)_2 + 3H_2 \rightarrow 2RH + 2H_2S$
Denitrogenation	$C_4H_4NH + 4H_2 \rightarrow C_4H_{10} + NH_3$
	$C_5H_5N + 5H_2 \rightarrow C_5H_{12} + NH_3$

2.1.2 Hydrotreating Unit

All Hydrotreating units have similar elements as showed in . First, the liquid feed is mixed to hydrogen gas and preheated in a heat exchanger and a furnace, and then the stream follows to a catalytic bed reactor. The reactor effluent is cooled down and the hydrogen-rich gas is separated in a high-pressure separator. Before recycling the hydrogen gas, hydrogen sulfide should be removed from the stream, using an amine gas treating. Afterwards, a part of the gas is purged, reducing the concentration of light hydrocarbons (C_1-C_4) in order to control the hydrogen gas pressure. Finally, the reactor liquid effluent is fractionated into product and the amine solution rich in the absorbed hydrogen sulfide gas is regenerated in the amine absorption unit.

Figure 2-1: Simplified Hydrotreating process flow

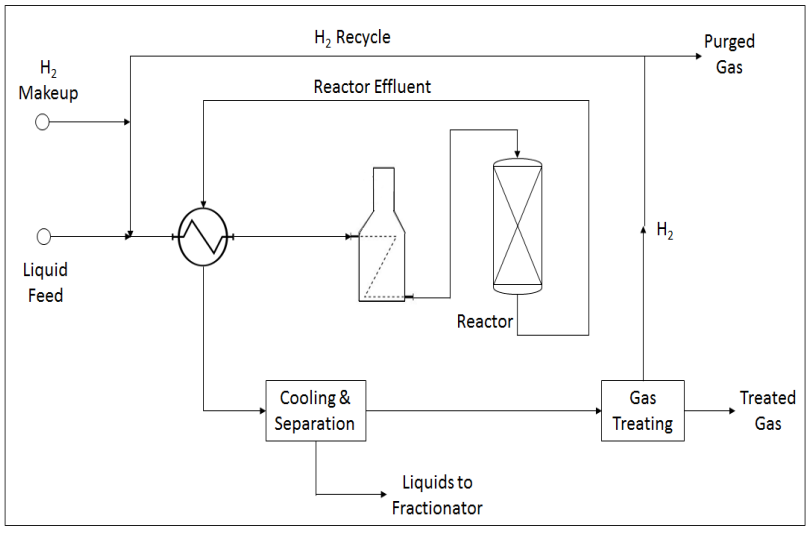

Source: (FAHIM, M. A.; AL-SAHHAF, T. A.; ELKILANI, 2012).

2.1.3 Amine Absorption Unit

The refinery process produces a large quantity of sour and acid gases as contaminants. Acid gases are formed by CO_2 and H_2S, sour gas contains sulfur compounds, such as carbonyl sulfide (COS) and mercaptans, Table 2-4. Both CO_2 and H_2S gas are harmful to environment and unsafe for people and should be removed and converted to a safer chemical.

Table 2-4: Typical acid and sour gas composition (FAHIM, M. A.; AL-SAHHAF, T. A.; ELKILANI, 2012).

Component	**Sour gas (% mole)**	**Acid gas (% mole)**
CO_2	8.50	18.60
H_2S	13.54	78.71
CH_4	77.26	1.47
C_2H_6	0.21	0.09
C_3^+	0.23	0.11
COS	0.02	0.05
RSH	0.01	0.04
H_2O	0.01	0.04
N_2	0.34	0.00

Acid gas contains mainly H_2S, Table 2-4. Hydrogen sulfide is a dangerous substance to people and also accelerates the corrosion process in equipment, and thus it should be treated through an absorption process. Absorption is a unit operation used to remove impurities (solute) from a gas stream, using a liquid solvent, which the solute is soluble. After that, the solute is recovered from the liquid.

Amines are a common solvent used in acid gases absorption process in refineries. A simplified amine absorption unit is presented in Figure 2-2. The unit contains an absorber and a stripper, where the former removes the solute from the gas stream and the latter is responsible for regenerating the solvent. The gas stream enters in the bottom of the absorber and the solvent enters in the top. Next, the resultant (rich) amine is directed to a regenerator, where the solute is removed. On the stripper bottom, the lean amine is recirculated to the absorber and the gas stream, on the stripper top, concentrated with H_2S, is routed to another unit to sulfur recovery.

Figure 2-2: Simplified Amine absorption unit process flow

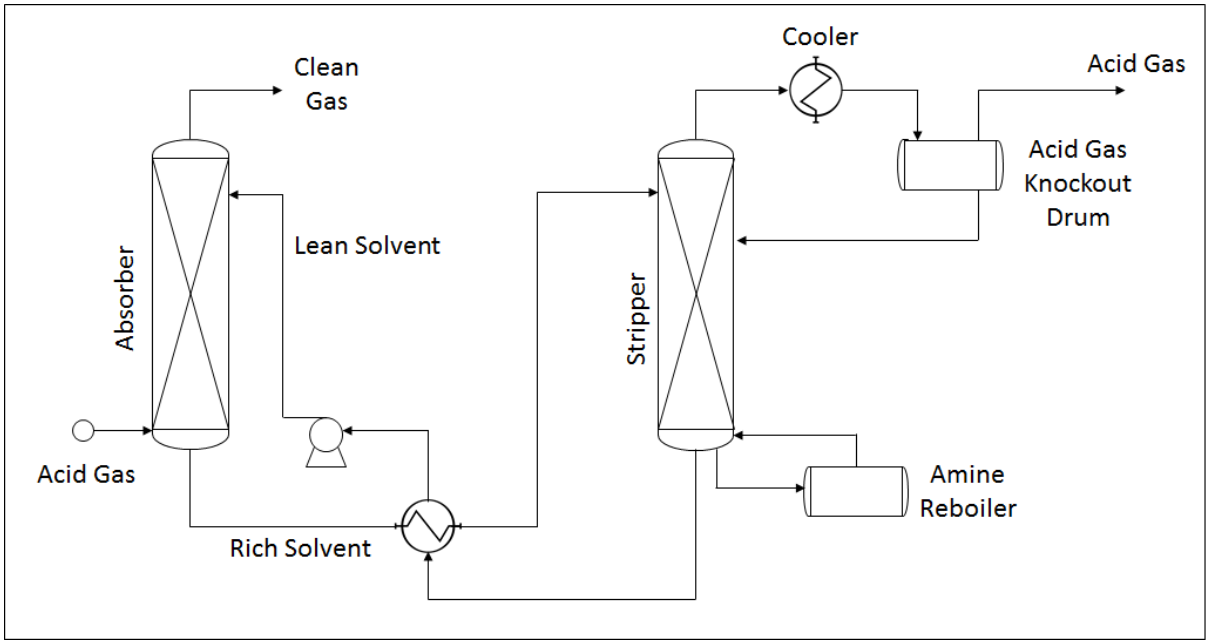

Source: (FAHIM, M. A.; AL-SAHHAF, T. A.; ELKILANI, 2012).

2.1.4 Sour water treatment

The oil refining process produces a large amount of sour water in distillation units, hydrocracker, hydrodesulfurization, amine regenerators and delayed cokers. The sour water streams are mixed, cooled and stored in a tank in the refinery. The main objective of the sour water treatment is the removal of H_2S and NH_3, since at certain temperatures and pressure, H_2S and NH_3 may combine to form solid ammonium bisulfide (NH_4HS), which can gradually obstruct pipes and equipment, and also cause corrosion (ZHU et al., 2016).

A process diagram flow for a Sour Water Treatment unit is presented in Source: . The feed from the sour water tank is heated up before entering the stripper. Ammonia and H_2S are removed from the water inside this equipment, producing off gas in the top and an effluent (stripped water) in the bottom. The stripped water can be reused in the process units or discarded.

Figure 2-3: Sour water stripping

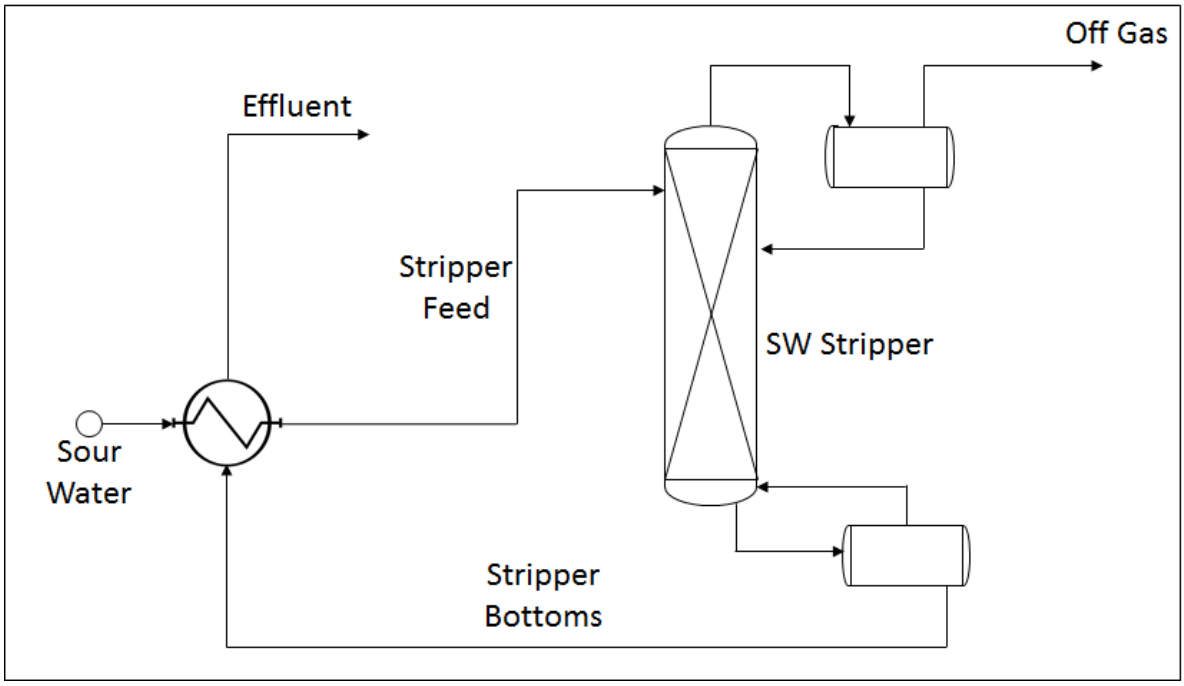

Source: (FAHIM, M. A.; AL-SAHHAF, T. A.; ELKILANI, 2012).

2.1.5 WSA Process

The Wet Gas Sulfuric Acid (WSA) process is a proprietary development by Haldor Topsøe A/S. The process converts the hydrogen sulfide into a commercial quality sulfuric acid and more than 60 plant worldwide have been using the technology (LAURSEN, 2007). The WSA process has a lower investment and has better heat economy than Claus plant (FAHIM, M. A.; AL-SAHHAF, T. A.; ELKILANI, 2010), besides the process is more versatile and admits a great variation in the feed composition (LAURSEN; KARAVANOV, 2006). Acid gas streams recovery from hydrotreating, amine absorption and sour water treatment units are sent to the WSA unit. In this unit, the combustion, condensation and hydration reactions take place (Table 2-5).

Table 2-5: Hydrogen sulfide gas conversion in a WSA/SNOX™ Plant (LAURSEN, 2007).

Combustion	$H_2S + 3/2O_2 \rightarrow H_2O + SO_2 + 518$ kJ/mole
Oxidation	$SO_2 + ½O_2 \leftrightarrow SO_3 + 99$ kJ/mole
Hydration	$SO_3 + H_2O \leftrightarrow H_2SO_{4(g)} + 101$ kJ/mole
Condensation	$H_2SO_{4(g)} + 0.17\ H_2O_{(g)} \leftrightarrow H_2SO_{4(l)} + 69$ kJ/mole

The WSA plant for H_2S gas is illustrated in . First, the acid gas is incinerated to produce SO_2. The heat produced by the combustion reaction is used to generate steam in a Water Heat Boiler (WHB). After leaving the WHB, the gas at a temperature close to 400°C, follows to a catalytic reactor, converting SO_2 to SO_3. As the oxidation reaction is exothermal, the gas is cooled down to benefit SO_3 production in the SO_2/SO_3 equilibrium. In the last stage, the gas is cooled to 300°C and the SO_3 reacts to water, yielding H_2SO_4. In the WSA condenser, the gas flows upwards inside the tubes cooled by the ambient air. H_2SO_4 flows down and accumulates in the condenser bottom, where is cooled to 30-40°C and is pumped to storage (LAURSEN; KARAVANOV, 2006).

Figure 2-4: WSA process for H2S gas

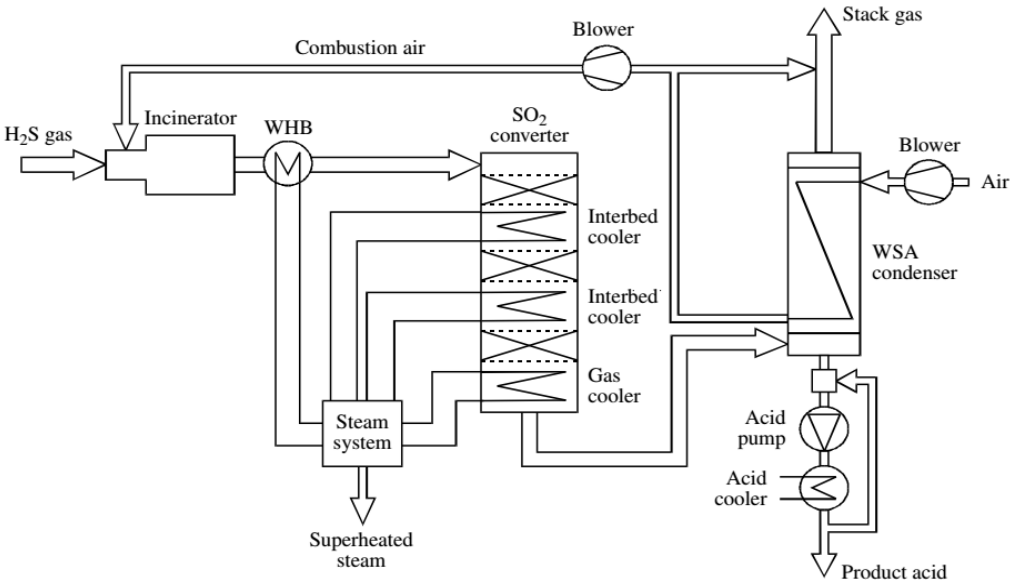

Source: (LAURSEN; KARAVANOV, 2006).

2.2 Risk Assessment

Hazard can be defined as one or more physical conditions that can cause harm on people, property and/or environment. Risk is a function of accidental scenarios frequency and the magnitude of the physical effects resulting from these scenarios (MILAZZO; AVEN, 2012).

The release of hazardous chemicals can cause rare, but catastrophic accidents and safety measures should be specifically implemented to mitigate such risks. Hence, making a good risk

assessment is the essential step to effectively prevent accidents (VILLA et al., 2016). Risk assessment is a combination between risk analysis and risk evaluation, where risk analysis is a proactive approach used to identify hazards, determine consequences of the event and calculate frequencies of occurrence of this event, whereas risk evaluation is a process to decide if the risks identified in the risk analysis are tolerable taking into consideration some factors such socioeconomic and environmental aspects (RAUSAND, 2006).

A risk analysis usually considers the structure below (TNO, 2005a; KHAN; RATHNAYAKA; AHMED, 2015) :

- Hazard identification: a brain storming analysis to identify possible accidental scenario, causes and consequences;
- Consequence analysis: determination of the potential physical effects and damage which can be caused by these effects;
- Determination of the probability of occurrence of the accident;
- Risk calculation and evaluation.

Each step uses techniques summarized in . The Preliminary Hazard Analysis (PHA) and HAZOP (Hazard and Operability Studies) are two of the techniques used for identifying hazards and analyze accidental scenarios. The quantitative AQR technique simulates the scenarios identified by the qualitative risk techniques and estimates the consequences of the physical effects. Fault tree and event tree techniques (MARHAVILAS; KOULOURIOTIS; GEMENI, 2011) are used to estimate the frequencies of occurrence of these scenarios.

Figure 2-5: Classification of the main risk analysis techniques.

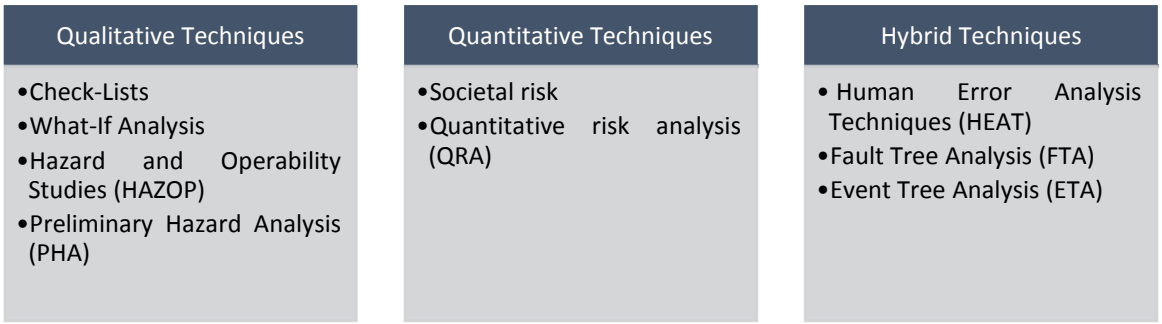

Adapted from (MARHAVILAS; KOULOURIOTIS; GEMENI, 2011).

The PHA focuses on every hazardous event caused by intrinsic failures of equipment, instruments and materials, and human errors. Moreover, it presents the causes and consequences of these hazards, as well as the expected severity (RAUSAND, 2006; CETESB, 2014). Table 2-6 shows the severity categories considered in a PHA, while Table 2-7 consists of a worksheet used for PHA.

Table 2-6: PHA severities

Rank	**Severity Class**	**Description**
I	Negligible	No injuries or first aid case
II	Minor	Mild injuries
III	Major	Serious injuries
IV	Critical	Single fatality
V	Catastrophic	Multiple fatalities

Source: This research, 2017.

Table 2-7: Sample PHA Worksheet

Facility:				
Process Unity:				
System element description:				
Hazard	Cause	Consequences	Severity Class	Prevention measures and Risk-reducing measures

Source: This research, 2017.

Quantitative risk analysis (QRA) methods provides numerical information about probabilities and consequences. The information obtained is used to create risk maps, which are useful for the decision-making process and development of the emergency plan (TNO, 2005).

The results of a QRA are the individual and societal risk (TNO, 2005). Individual risk is the probability of an individual death due to one or more accidental scenarios within a year (RAUSAND, 2006; GAI et al., 2017), and is calculated for several geographic points (x, y) around the facility. The individual risk at each point considers the effects of every accidental scenarios altogether.

The results obtained in the QRA (the concentration of toxic agents in time and space) will serve as input data for the calculation of individual risk. Thus, the individual risk due to

the accident of type i in the location (x, y) is presented by equation (2.1), where P_f is the probability of failure and $P_{d/f}$ is the probability of individual death because of this failure (GAI et al., 2017). The total individual risk or total localized individual risk (RAUSAND, 2006) is given by the sum of the risks of each accidental scenario that affects the location (x, y), according to equation (2.2) (RAUSAND, 2006; ZHOU; LIU, 2012).

$$IR_{x,y,i} = P_f \times P_{d/f} \quad (2.1)$$

$$IR_{x,y} = \sum_{i=1}^{n} IR_{x,y,i} \quad (2.2)$$

- $IR_{x,y}$ = Total Individual Risk at location (x, y) (fatality expected in a year);
- $IR_{x,y,i}$ = Individual Risk at x, y coordinate due to accident of type i (fatality expected in a year);
- n = total number of accidental scenarios considered in the analysis.
- i = 1, 2, …, n.

Gai et al. (2017) and Cetesb (2014) apply the same evaluation to judge the tolerability of the risk. The risk is divided in three areas:

1. Acceptable area: $IR < 1 \times 10^{-6} year^{-1}$;
2. Area where the risk can be considered affordable, however it could be reduced (ALARP – "As Low As Reasonably Practicable"): $1 \times 10^{-6} year^{-1} \leq IR \leq 1 \times 10^{-5}$
3. Non-acceptable area: $IR > 1 \times 10^{-5} year^{-1}$

2.3 Evacuation Models

There are several types of protective actions that can be implemented in cases of major accidents such as evacuation, shelter for the population in specific constructions, respiratory protection, use of protective clothing, use of prophylactic drugs and antidotes (GEORGIADOU et al., 2010). Evacuation is the most complex mitigation measures and it needs a precise planning and allocation of resources. In addition, this action presents a greater implicit risk, since it can increase the probability of accidents during the urgent collective movement and patrimony abandonment. However, evacuation is an efficient measure to reduce the number of

fatalities after the leakage of hazardous substances being more effective in continuous leakage than in instantaneous leakage (DUARTE, 2002).

There are several mathematical models to simulate evacuations that can be macroscopic or microscopic. Macroscopic models are based on network models, but ignore individual behavior in emergency conditions. Microscopic models, however, consider individual behaviors and interactions in the evacuation process (GAI et al., 2017).

Different studies have been developed in different perspectives in evacuation planning. For example, Sorensen, Shumpert & Vogt (2004) present some methods to prepare information for an efficient decision making in an emergency case. The authors defend that does not exist a simple technical decision-making method to choose the protective actions for every accidental scenario. So, the decision models must be coupled with decision support tools: libraries of accident scenarios coupled with protective action look-up tables or use simulation models to estimate the optimum decision given a specified decision objective.

In the perspective of optimization problems, Shen *et al*. (2015) proposes a mono-objective optimization problem to minimize the health injury to the workers during an evacuation due to a toxic release in a chemical industrial park. The effect in people is calculated using a variable based on toxic load defined as a product of concentration of the toxic gas and time of exposure. The velocity of the evacuees is considered constant and the congestion of the roads is ignored, these two assumptions could not be applied in real situations. The problem is solved using a modified YEN's K-shortest path algorithm to calculate the best route.

In the perspective of multi-objective optimization problems there are some important studies to mention. Georgiadou *et al.* (2010) present a methodology for multi-objective optimization evacuation planning that aims to minimize the health effects in the population due to the exposure to hazardous materials and minimize the socioeconomic costs related to the evacuation response planning. The problem is solved using SPEA II, the Strength Pareto Evolutionary Algorithm.

Saadatseresht, Mansourian and Taleai (2009) propose a three-step approach for evacuation planning. In the first step, the safe areas for evacuation are selected. In the second step, the optimal path from the building blocks to the safe areas are found. Finally, the final step is a multi-objective optimization problem that aims to find the optimal safe area for each

building block. The problem is solved using the NSGA-II (*Nondominated Sorting Genetic Algorithm II)* in a GIS (Geographical information system) environment.

Li *et al.* (2010) present a model based on genetic algorithm for emergency evacuation planning in public spaces (stadium). The model minimizes three objectives: total evacuation time, total travel distance of all the evacuees and the congestion during the evacuation. The authors also considered a constant velocity for the individuals and the MOP is solved with the NSGA-II.

Melo (2015) developed a model of crowd evacuation simulation in emergency situations adaptable to different scenarios using cellular automata. The model was applied to an auditorium where its characteristics were compared and adapted to the NBR 9077: 2001- Building Emergency Exits. The author shows the average evacuation time for different positions of the door.

Ikeda & Inoue (2016) presented a method for evacuation planning during natural disasters that considers GPS data and accelerometer data from people's smartphones. In order to minimize the evacuation distance, evacuation time and safety of evacuation route, a MOGA is used. The evacuation time is calculated by adding all average walking time of links that compose the route. A function to evaluate the safety during evacuation is also proposed. The safety evaluation is based on the relation between the walking speed and the pedestrian traffic, so the roads with higher traffic and higher individual speed are considered to be safer.

Gai *et al.* (2017) proposes a multi-objective model to minimize the total time of evacuation and the individual risk along the evacuation route in a toxic cloud release scenario. The authors considered that the individual velocity during evacuating is not a constant and it will decrease with the extension of disaster in time and space (YUAN; WANG, 2009). The MOP is solved using two heuristic algorithms based on a modified Dijkstra algorithm.

Santos (2016) and De Lima e Silva (2017) solve a similar MOP for different toxic release scenarios using the Modified Dijkstra Algorithm from Gai *et al.* (2017). De Lima e Silva (2017) identifies and assess the risk of the atmospheric distillation unit, delayed coking unit and hydrotreating unit in an oil refinery. The author considers a hydrogen sulfide release for each scenario simulated. Both Santos (2016) and De Lima e Silva (2017) also presents a sensitive analysis for the parameters used to estimate the individual velocity.

2.4 Multi-objective Optimization

A multi-objective optimization problem consists in finding a decision variable vector that optimizes a vector of objective functions, satisfying a vector of constraints. Optimizing a multi-objective problem has a different idea from optimizing single objective functions. Whereas in a single optimization problem we may find the solution by comparing different values of a unique objective function for different decision variables vectors, a multi-objective problem presents a great number of set of solutions, which when evaluated, generate vectors whose components satisfy an acceptable level for the decision maker. Therefore, the goal in a multi-objective optimization problem is to find good trade-offs instead of a single solution (COELLO COELLO; LAMONT; VAN VELDHUIZEN, 2007).

The notion of optimum used for multi-objective problems is known as Pareto Optimum. Pareto Optimal is defined as a vector of decision variables $\boldsymbol{x}^* \in \Omega$, where there is no other vector of decision $\boldsymbol{x} \in \Omega$ for which $\boldsymbol{v} = F(\boldsymbol{x}^*) = \big(f_1(\boldsymbol{x}^*), \dots, f_k(\boldsymbol{x}^*)\big)$ dominates $\boldsymbol{u} = F(\boldsymbol{x}) = \big(f_1(\boldsymbol{x}), \dots, f_k(\boldsymbol{x})\big)$. A decision vector $\boldsymbol{x}^*$ is said to dominate a decision vector $\boldsymbol{x}$ if and only if $f_i(\boldsymbol{x}^*) \leq f_i(\boldsymbol{x})$ for all $i = 1, \dots, k$ and $f_j(\boldsymbol{x}^*) < f_j(\boldsymbol{x})$ for at least one j (if all objective functions are for minimization). The set formed by all the feasible non-dominated decision vectors is called **Pareto Optimum Set** and the objective functions plotted at the objective space are called **Pareto Front** (COELLO COELLO; LAMONT; VAN VELDHUIZEN, 2007; GEORGIADOU et al., 2010). As the number of Pareto Optimal solutions is huge, maybe infinite, for most of the problems, a good multi-objective algorithm must find a set of solutions that better represents the Pareto Optimal Set (KONAK; COIT; SMITH, 2006).

2.4.1 Genetic algorithms for Solving Multi-Objective Problems

Genetic algorithms (GA) are search methods that are based on mechanisms of evolution and natural selection. The concept of GA was developed by Holland and his colleagues in the 1960s and 1970s. In nature, more adapted species are more likely to pass their genes to future generations via reproduction, otherwise they are extinguished by natural selection. Over time, species that have the best set of genes become dominant in the population.

Sometimes, minor changes, called mutations, can occur in the genes during the process. If mutation brings features that aid in the survival of the individual, a new, more evolved species

emerge. However, changes, which bring some disadvantage to this individual, will cause it to be eliminated by natural selection (KONAK; COIT; SMITH, 2006).

In GA terminology, the solution vector is called individual or chromosome. Chromosomes are made up of discrete units called genes. A scalar value, called fitness, is assigned to every individual. This scalar value will be considered as a parameter of quality during the optimization process (GEORGIADOU et al., 2010). GA operates on a group of chromosomes, called population, which is usually randomly initiated. As the search progresses, the population includes even better solutions, and eventually converges, meaning that it is dominated by a single solution (KONAK; COIT; SMITH, 2006).

GA uses two operators to generate new individuals: crossover and mutation. The former is the most important operator of GA (KONAK; COIT; SMITH, 2006), and connects parts of parent chromosomes to generate new chromosomes (children). The best parents, chosen according to their fitness, are preferably selected among existing chromosomes in the population, so that children can inherit the good genes from these adapted parents. During the crossover step it can be used different GA selection procedures such as proportional selection, ranking and tournament selection. The iterative application of the crossover operator aims to make the best chromosomes appear more frequently in the population, eventually leading to convergence for a good global solution (KONAK; COIT; SMITH, 2006).

The mutation operator in turn introduces random changes in the characteristics of the chromosomes. Mutation plays a critical role in GA. As the crossover causes the population to converge, making the chromosomes in the population more similar, the mutation reestablishes genetic diversity back to the population. This diversity prevents the algorithm from converging very fast and prevents the solution from stabilizing in local minimum regions (KONAK; COIT; SMITH, 2006).

MOGA is an approach to multi-objective optimization problems using GA. This algorithm can reach all the set of Pareto optimal solutions at the same time because GA works simultaneously with multiple points (IKEDA; INOUE, 2016). Moreover, MOGA is essential to problems with a huge solution set, for which exact methods, like the exhaustive one, are very time-consuming and can require a prohibitively long time to give a solution. For a more complex network, as expected in a large facility as a refinery, an exact method can be

impracticable, and then a heuristic method must be used. For example, Table 2-8 presents how the number of possible solutions increases, increasing the number of nodes in a complete graph, a simple undirected graph in which every pair of distinct vertices is connected by a unique edge.

Table 2-8: Maximum number of paths between two nodes in a complete graph for different number of nodes.

Number of Nodes	Maximum number of paths between two nodes
10	109,601
20	17,403,456,103,284,400
30	828,772,446,866,981,000,000,000,000,000

2.5 ALOHA® Software and Level of Concern (LOC)

ALOHA® is a hazard modelling program that uses data on actual or potential release of a chemical and estimates threat zones for different types of hazards such as: toxic clouds, cloud fire, BLEVEs (Boiling Liquid Expanding Vapor Explosions), jet fire, fire in puddle and explosions (JONES, R., W. LEHR, D. SIMECEK-BEATTY, 2013).

A toxic threat zone is an overhead view of the area where the concentration is predicted to exceed the Level of Concern (LOC) in a period of time after a release begins. A toxic LOC shows the level (limit of concentration) of exposure to a toxic chemical could harm people if they breathe it in for a defined period of time. Usually, a lower LOC means that the substance is highly toxic to inhalation. ALOHA uses the most common public exposure guidelines: AEGLs (Acute Exposure Guideline Levels), ERPGs (Emergency Response Planning Guidelines), and TEELs (Temporary Emergency Exposure Limits). They are some main differences between theses exposure guidelines, however at every general level the tiers are similar: the first one is a concentration level that causes minimal health effects, the second tier represents an escape impairment concentration level and the third tier is a fatal concentration level. For example, Table 2-9 shows the definition for each level of AEGL.

Table 2-9: AEGLs definitions (NOAA, 2017a)

Acute Exposure Guideline Levels (AEGLs)	**Definition**
AEGL-3	People could experience life-threatening health effects or death.
AEGL-2	People could experience irreversible or other serious adverse health effects or a diminished ability to escape.
AEGL-1	People could experience notable discomfort, irritation, however, the effects are reversible and not disabling.

In Figure 2-6, there is a threat zone picture presenting the three LOCs for a toxic chemical release. The area in red has a concentration value that exceeds 20 ppm corresponding to a AEGL-3 of the chemical release simulated. A person inside this area has a high risk of death. The area in orange and yellow represent the AEGL-2 and AEGL-1 respectively. Moreover, the picture shows an area where the AEGL-1 can be achieved due to changes in the wind direction. The threat zone picture shows the higher concentrations achieved during the entire simulation, concentration values presented in the figure could not be the same during all the period of time of the release.

Figure 2-6: ALOHA threat zone picture presenting the three levels of AEGL

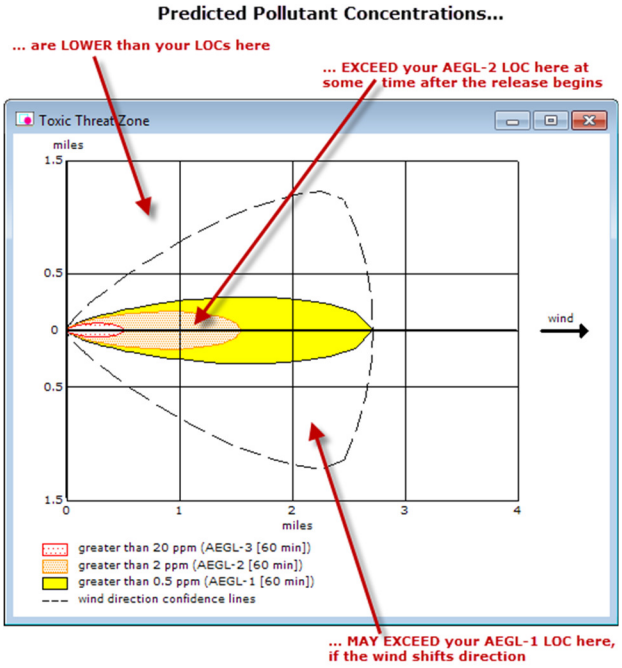

Source: (NOAA, 2017b).

Most exposure guidelines are based on the period of exposure. The AEGL has information about different period of time. The values for the chemical hydrogen sulfide is presented in Table 2-10.

Table 2-10: AEGL Values for Hydrogen Sulfide for different time of exposure

Classification	**10 min**	**30 min**	**1h**	**4h**	**8h**
AEGL-1 (Nondisabling)	0.75 ppm (1.05 mg/m^3)	0.60 ppm (0.84 mg/m^3)	0.51 ppm (0.71 mg/m^3)	0.36 ppm (0.50 mg/m^3)	0.33 ppm (0.46 mg/m^3)
AEGL-2 (Disabling)	41 ppm (59 mg/m^3)	32 ppm (45 mg/m^3)	27 ppm (39 mg/m^3)	20 ppm (28 mg/m^3)	17 ppm (24 mg/m^3)
AEGL-3 (Lethality)	76 ppm (106 mg/m^3)	59 ppm (85 mg/m^3)	50 ppm (71 mg/m^3)	37 ppm (52 mg/m^3)	31 ppm (44 mg/m^3)

Source: (NATIONAL RESEARCH COUNCIL, 2010)

3 PROPOSED METHODOLOGY

This dissertation is an applied research, where a MOGA was implemented to find the non-dominated solutions of an evacuation route optimization problem in a refinery. The MOGA implemented was validated with the results obtained by the exhaustive method. The study had a qualitative and quantitative approach. The dissertation has the form of a case study, where different accidental situations in oil processing units were considered.

3.1 Evacuation network

The evacuation route network is illustrated in , and has 20 nodes that correspond to processing units and other strategic places in a refinery. The starting point of the evacuees and the accidental scenario may happen in any node (1 to 19) except in the safety area (node 20). The scale map is 1:10000, which means 1 cm on the map equals 100 m on the ground.

Figure 3-1: Emergency evacuation route network

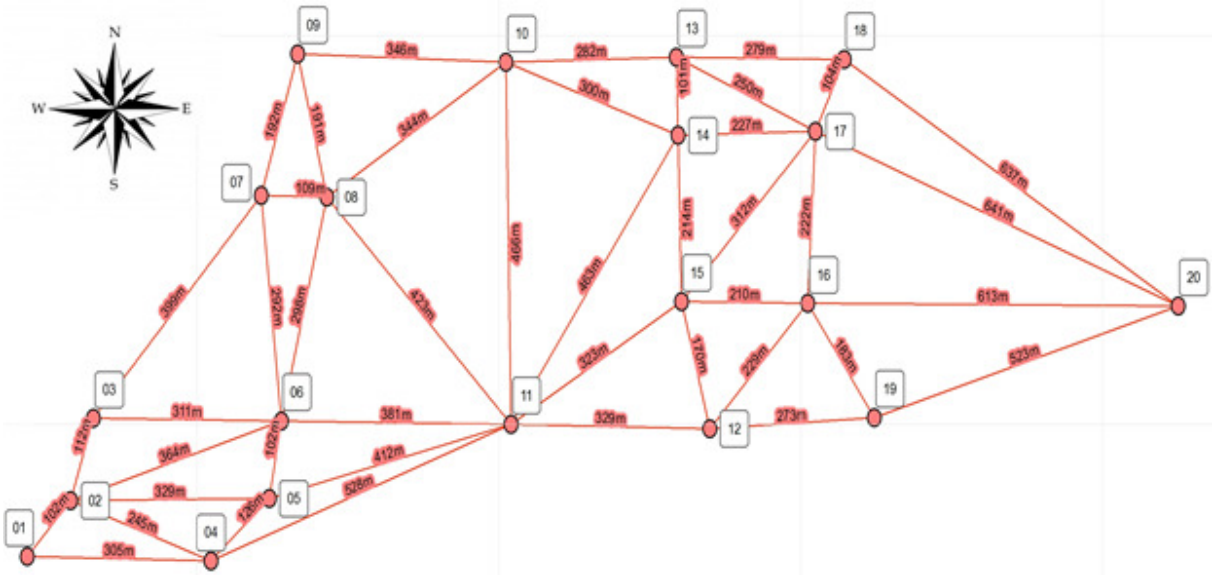

Adapted from (DE LIMA E SILVA, 2017)

3.2 Modeling accidental scenarios

The hazardous events identified in the PHA with a toxic cloud release as consequence and a severity class higher than major (III) were selected to be modeled in ALOHA® software to estimate the concentration values in time for each node in . All the scenarios were simulated in the same conditions presented in Table 3-1.

Table 3-1: Site information, weather conditions and ground roughness

Building Type	**Single storied building**
Building Surroundings	Unsheltered surroundings
Wind speed	3 m/s
Wind direction	WSW (west south-west)
Wind measurement height	10 m
Ground Roughness	Urban or forest
Cloud Cover	Clear
Air Temperature	25°C
Stability Class	D
Inversion Height	No inversion
Humidity (Relative)	80%

Adapted from (DE LIMA E SILVA, 2017)

Each release scenario corresponds to a release of hydrogen sulfide gas due to pipe rupture in the Amine Absorber, Sour Water Treatment and WSA units (Table 3-2).

Table 3-2: Release scenarios modeled

Process Unit	**System element description**
Amine Absorber Unit	Regenerator top outlet pipe
Sour water treatment Unit	Sour water stripper top outlet pipe
WSA Unit	Knock out drum acid gas outlet pipe

The scenario selected from the amine absorber unit is the outlet pipe, 14”, from the top of the regenerator (a stripper with a reboiler), which produces “lean” amine that is recycled for reuse in the absorber. The stripped overhead gas is concentrated H_2S. The stripper has 28 m of length and a diameter of 1.65 m.

Table 3-3: Amine absorption unit scenario input information

Source in ALOHA®	Chemical	Temperature	Pressure	Type of leakage	Opening diameter
Tank	Hydrogen Sulfide	110 ºC	2.15 kgf/cm²	Through a short pipe	14 inches

The scenario selected from the sour water treatment unit is the outlet pipe, 10", from the top of the splitter, which produces stripped water in the bottom to be reused in the process. The off-gas stream from the splitter top can be directed to a sulfur recovery unit or to the torch system. The stripper has 45.5 m of length and a diameter of 2.55 m.

Table 3-4: Sour water treatment unit scenario input information

Source in ALOHA®	Chemical	Temperature	Pressure	Type of leakage	Opening diameter
Tank	Hydrogen Sulfide	120 ºC	2.05 kgf/cm²	Through a short pipe	10 inches

Finally, the scenario selected from the WSA unit is the outlet pipe, 14", from the top of the feed knock out drum. The knock out drum is used to remove any liquid droplets presented in the gas stream. The knock-out drum has 3.5 m of length and a diameter of 0.8 m.

Table 3-5: WSA unit scenario input information

Source in ALOHA®	Chemical	Temperature	Pressure	Type of leakage	Opening diameter
Tank	Hydrogen Sulfide	40 ºC	1.70 kgf/cm²	Through a short pipe	14 inch

Another assumption considered in the modelling is that all the leakage scenarios are interrupted after a period of time of 2 minutes because of a blocking system actuation where the detection of leakage and closure of the valves are fully automatic (TNO, 2005).

3.3 Problem Statement and Formulation

The objectives of the optimization problem are to minimize the individual risk and evacuation time along the escape route. The use of genetic algorithms has some advantages in relation to the weighted sum method used by Gai *et al.* (2017). In fact, GA finds various members of the Pareto optimal set in a single run of the algorithm, whereas the weighted sum method needs to perform several separate runs with varied weighting coefficients (COELLO COELLO; LAMONT; VAN VELDHUIZEN, 2007).

The toxic concentration in time and space were calculated using ALOHA® (*Areal Locations of Hazardous Atmospheres*) software for accidental scenarios with the PHA severity equal or higher than III (Table 2-6). The probability of an individual death due to a exposure of a toxic, $P_{d/f}$, is related to the Probit (Pr) equation and the error function (*erf*), equation (3.1) (GAI et al., 2017).

$$P_{d/f} = 0{,}5\left[1 + erf\left(\frac{|Pr - 5|}{\sqrt{2}}\right)\right] \tag{3.1}$$

The Probit equations estimate the probability of fatality of an individual by the combination of concentration and duration of exposure and has the form of equation (3.2). In this equation, *Pr* represents the Probit variable; *a, b* are constants that depend on the chemical and *D* is the chemical lethal dose. For toxic substances, the lethal dose is calculated from the relation presented in equation (3.3), where *C* is the toxic concentration, *n* is a constant that also depends on the chemical and the time of exposure (TNO, 2005; GAI et al., 2017).

$$\mathrm{Pr} = a + b\ lnD \tag{3.2}$$

$$D = C^n t_e \tag{3.3}$$

The results of toxic concentration as a function of location (*x, y*) at time *t*, C*(x,y,t)* obtained by the simulation of the toxic cloud dispersion (ALOHA® software) will be used to estimate the toxic dose value, equation (3.4), that is the dose an individual is exposed while traveling the distance between the nodes *i* and *j*, the departure and arrival node respectively.

$$D_{ij} = \int_{t_i}^{t_j} C^n(x, y, t)dt \tag{3.4}$$

The lethal dose for the entire evacuation route (R) were calculated according to the equations below, equations (3.5), (3.6), (3.7) and (3.8):

$$D(R) = \sum_{i=1}^{n}\sum_{j=1}^{n} z_{ij}D_{ij} \tag{3.5}$$

Subject to

$$\sum_{j=1,j\neq i}^{n} z_{ij} - \sum_{j=1,j\neq i}^{n} z_{ji} = \begin{cases} 1, i = 1 \\ -1, i = n \\ 0, \text{otherwise} \end{cases} \tag{3.6}$$

$$\sum_{j=1,j\neq i}^{n} z_{ij} = \begin{cases} 0, i \neq n\ (i\ does\ not\ belong\ to\ route\ R) \\ 1, i \neq n\ (i\ belongs\ to\ route\ R) \\ 0, i = n \end{cases} \tag{3.7}$$

$$z_{ij} = [0,1] \quad i,j \in \{1,2,\dots,n\}, \tag{3.8}$$

where z_{ij} is a decision variable; for $z_{ij}=0$ arc (i, j) is not included in the evacuation route and for $z_{ij}=1$ the arc is included in the route, according to equation (3.8). Equation (3.6) restricts the departure and arrival nodes in evacuation route R. Equation (3.7) avoids circles formation in evacuation route R, because, for every node (except the destination node) there is none or only one edge starting from node *i* to node *j (*the sum of the decision variables is equal to 1 if the node *i* belongs to route R or the sum is equal to zero if node *i* does not belong to the route*)* and there is not any edge starting from the destination node *n.*

For the evacuation time calculation, it is known that the individual's travel speed at the arcs of the evacuation route tends to decrease with time and distance from the origin and the present location of the individual (YUAN; WANG, 2009; GAI et al., 2017). Consequently, equation

(3.9) defines the individual speed between nodes *i* and *j* under the disaster conditions, $u_{ij}(t)$ (YUAN; WANG, 2009; GAI et al., 2017).

$$u_{ij}(t) = u_{ij}^{0} \,.\, \alpha_{ij} \,.\, e^{-\beta_{ij} t}, \tag{3.9}$$

where u_{ij}^{0} is the initial travel speed on arc (*i, j*) under normal conditions, α_{ij} and β_{ij} are the travel speed parameters that affects $u_{ij}(t)$ and, as a result, the travel time. The factor α_{ij} reflects the direct influence of the accident in travel conditions on arcs. Small values of α_{ij} means the disaster has a high influence in the evacuation speed. The parameter β reflects the accident influence after a period of time: larger values of β, decreases faster the travel speed, indicating a greater extent of the accident (GAI et al., 2017). The values of these decay parameters can be estimated from the distance between the nodes *i* and *j* and the origin of the accident, the type of accidental scenario, path vulnerability etc. (YUAN; WANG, 2009; GAI et al., 2017). Then, the travel time on arc between nodes *i* and *j*, t_{ij}, is calculated using equations (3.10) and (3.11), where l_{ij} is the arc length:

$$\int_{t_i}^{t_j} u_{ij}(t)dt = l_{ij}\,, 0 < i < j \leq n, \tag{3.10}$$

$$t_{ij} = t_i - t_j. \tag{3.11}$$

Finally, the optimization problem is formulated below, where equation (3.12) minimizes the total travel time along an evacuation route and (3.13) minimizes the individual risk along this evacuation. The optimization problem is subject to the constraints already presented in equations (3.6), (3.7) and (3.8).

$$min\, T(R) = \sum_{i=1}^{n}\sum_{j=1}^{n} z_{ij} t_{ij} \tag{3.12}$$

$$\min IR(R) \tag{3.13}$$

3.4 Multi-Objective Genetic Algorithm

The GA algorithm operators presented in this work produces only feasible solutions. According to LINS (2013), generating only feasible solutions prevents MOGA to reach unfeasible locations, besides the use of penalty functions is unrequired.

In short, the whole procedure of MOGA involves an initial population (*P)* with *N* feasible individuals, see . First, the fitness value of each individual is evaluated, the individuals are compared to each other, and then separated in dominated and non-dominated solutions. The dominated solutions are eliminated from *P* and the non-dominated ones are used to update an auxiliary population, P_{aux}. The update step ensures that only non-dominated individuals will be stored in P_{aux}. The crossover and mutation operators generate new individuals (children) and the parents are replaced by them in the population. Each step is described in more details in the next topics.

Figure 3-2: MOGA algorithm

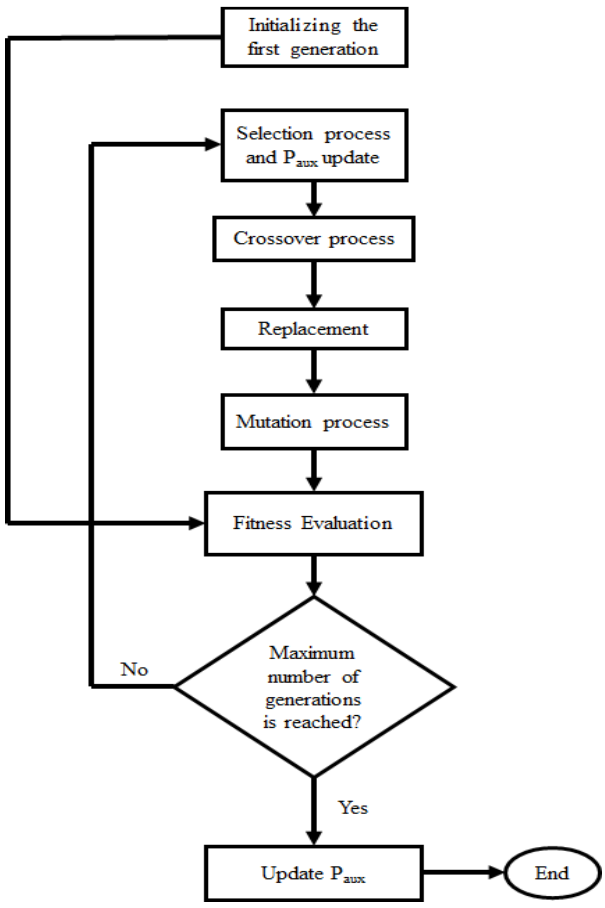

3.4.1 Individual Representation

The individual representation is given by an integer vector formed by a combination of ones and zeros. Each element represents an arc in the emergency evacuation network (). If the element is equal to 1 the arc belongs to the evacuation route, otherwise the arc does not belong to the evacuation route.

As an example, the left side of illustrates an evacuation route in an emergency evacuation network with 5 nodes and 7 arcs. An accident happens in node 1 and the starting point of evacuation is at the same node. The safety zone is located at node 5. A possible evacuation route is also presented: **1-2-4-5**. The evacuation route will be represented as the integer individual in the right side of .

Figure 3-3: An emergency evacuation route (left) and its individual representation in GA (right)

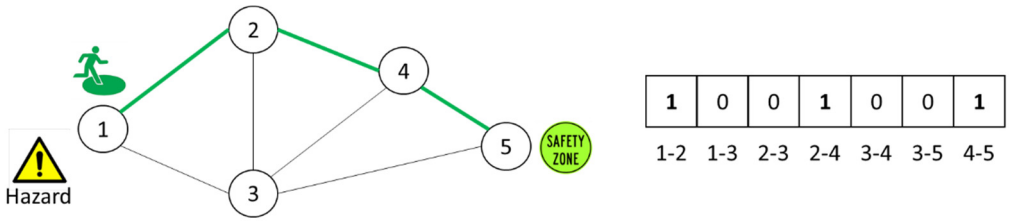

3.4.2 Initializing the first generation

The initial population P with N individuals is generated by randomly sampling edges that are connected together and form a path between the evacuation and safety point (node 1 and node 20 in). First, the current node algorithm chooses randomly an edge (i,j) in a set S(i) with all the edges that contains the start point as the current node i. For example in the start point is the node 1, so S(1) = {(1,2);(1,4)}. After that, the current node is updated to the node connected to the start point. Then, the algorithm finds all the possible edges that contains the current node *i*, updating the set S(*i*). Finally, the same procedure is repeated until the safety point, node 20, is reached. The presents the pseudocode:

Figure 3-4: Pseudocode of the proposed procedure to generate initial population

```
Procedure GENERATE INITIAL POPULATION
  i ⟵ Start Node
  individual[Ne] ⟵ {0,0,…,0} generate a vector individual with zeros
  while size of P < N do
     while i ≠ Final Node do
        Update S(i)
        edge(i,j) ⟵ an edge chosed randomly from S(i)
        pos ⟵ position in the individual of edge(i,j)
        individual[pos] ⟵ 1
        i ⟵ j
    if individual does not exist in P
      Add individual in P
End Procedure
```

3.4.3 Calculating fitness

Individuals fitness is calculated for each objective function: evacuation time and individual risk as presented in section 3.3. During calculation, the individual feasibility is checked although all the genetic operators (generation of the first population, crossover and mutation) generates only feasible individuals.

3.4.4 Selection and update of the auxiliary population

The selection step is responsible for choosing possible non-dominated individuals from the population to participate in an auxiliary population, considering their fitness values (section 3.3). The dominated individuals are removed from the population and the auxiliary population can be updated or not with the remaining individuals, according to the procedure described below (LINS, 2013):

- If a possible solution from the population is dominated by some individual in the auxiliary population, it is discarded;
- If a possible solution from the population dominates individuals in the auxiliary population, all dominated solutions are removed from the auxiliary population and a copy of the possible solution is stored in the auxiliary population;
- If a possible solution from the population is not dominated by individuals in the auxiliary population, the individual is included in the auxiliary population.

As the population decreases due to the elimination of non-dominated solutions, some individuals are randomly selected from the auxiliary population to be included in P in order to maintain the total number of individuals (*N*).

3.4.5 Crossover and Replacement

After the selection step, a random number in the [0,1] interval is assigned to each individual in *P*. The individuals with a number less than the crossover probability will participate in the crossover process (a copy of the individual is inserted in the set *Cross)*. A pair of individuals from the set *Cross*, the parents, is randomly selected and they have some positions exchanged. To guarantee the generation of feasible individuals, only the parents with the same node in common participate in the crossover, if they do not have nodes in common the children will be a copy of their parents. In the algorithm, , the nodes in common are found and the first position where the common node appears in the individual as a start point is included in the set *pos*. The parents exchanged theirs contents in the positions of the set *pos*. Finally, the algorithm returns the modified parents according to the replacement strategy "children replace parents".

Figure 3-5: Pseudocode of the proposed crossover procedure returning only feasible individuals

Procedure CROSSOVER
for $j = 1, \dots, N$ **do**
⇒ $select \longleftarrow random[0,1]$
if $select \leq p_{cr}$ **then**
⇒ $P[j]$ is inserted into $Cross$
⇒ a pair of individuals, *parent1* and *parent2*, is randomly chosen from $Cross$
⇒ *pos* ⟵ the individual position of nodes in common between *parent1* and *parent2*
⇒ *parent1* and *parent2* exchanged their contents according to *pos*
⇒ Return *parent1* and *parent2*
End Procedure

An example is illustrated in , the parents $\mathbf{P_1}$ and $\mathbf{P_2}$ have two nodes in common, nodes 3 and 6. The algorithm finds the positions where the parents must exchange parts (between the 3-4 and 6-7 positions). The number of positions exchanged is defined by the number of nodes in common between the parents. At the end of the crossover process, after all individuals in the set *Cross* are verified and have their positions exchanged, all the children generated replaced their parents automatically.

Figure 3-6: An example of the crossover operation

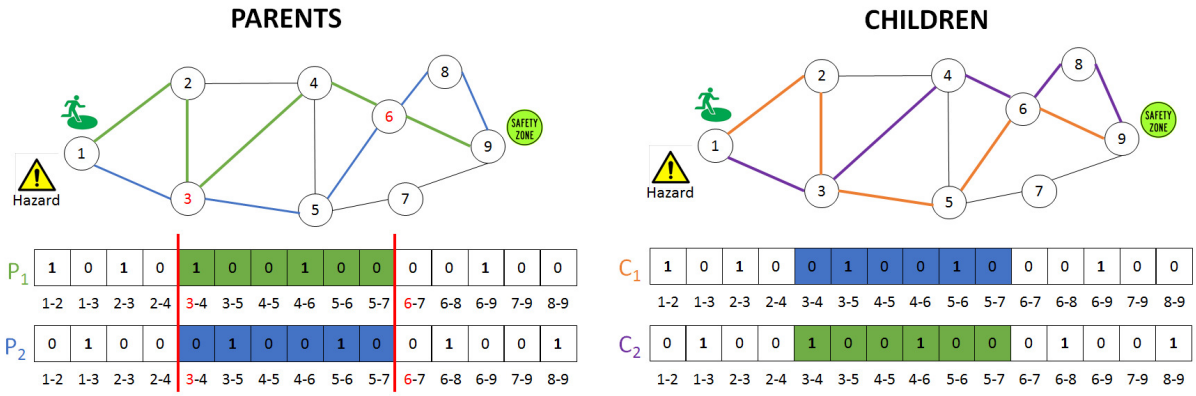

3.4.6 Mutation

Similar to the crossover operator, the mutation step assigns a random number in the [0,1] interval to each individual in P and select the individuals that will participate in the mutation stage. The individuals with a number less than the mutation probability will participate in the mutation process. In the mutation algorithm, , the individual selected is truncated in a position randomly chosen. So, the last node presented in the truncated individual is found and a new path is generated between that last node and the safety node.

Figure 3-7: Pseudocode of the proposed mutation procedure returning only feasible individuals

Procedure MUTATION
for $j = 1, \dots, N$ **do**
    $\Rightarrow select \longleftarrow random[0,1]$
    if $select \leq p_{mut}$ **then**
        old_P[j] = P[j]
        while P[j] = old_P[j] **do**
            $\Rightarrow pos \longleftarrow random[0, number\ of\ edges]$
            ⇒ P[j] ⟵ {P[pos], 0,..., 0}
            ⇒ Find the last node in P[j] and its position, *pos_n*
            ⇒ Generate a path between the last node in P[j] and the safety node: *Path*
            ⇒ P[j] ⟵ {P[*pos_n*], Path}
End Procedure

The example in illustrates all the mutation process. First, an individual selected, P_1, has a position randomly chosen. After that, a new path is generated from the last node available in the individual and the safety node. If the new individual C_1 is equal to the previous individual

P_1, the mutation process is redone, generating randomly a new position in P_1, otherwise the P_1 individual is replaced by C_1.

Figure 3-8: An example of the mutation operation

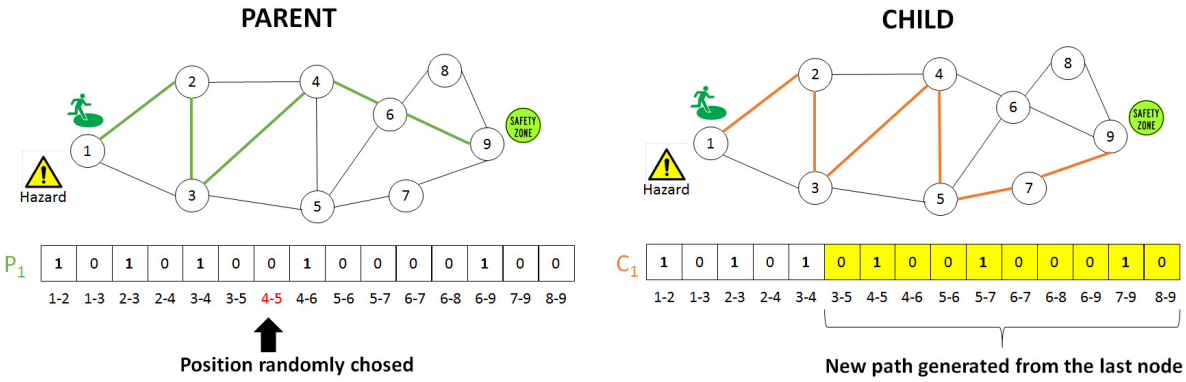

4 ANALYSIS OF RESULTS

4.1 ALOHA Results

The results obtained from the simulations of the accidental scenarios were represented in a toxic threat zone commented in section 2.5. All the simulations in ALOHA consider a maximum leaking time of 60 minutes, however as commented before in section 3.2, the maximum leaking time considered was 2 minutes. For all the simulations, the Probit Parameters used are listed on Table 4-1. For each scenario, it was specified three LOCs, the Acute Exposure Guideline Levels: AEGL-3, AEGL-2 and AEGL-1. The AEGL was chosen because it undergoes a careful review process, presents several concentration values for different exposure times and considers practically all the general public, including the most sensitive individuals such as infants, children, elderly, etc. (NOAA, 2017).

As most exposure guidelines are related to a time of exposure, ALOHA® recommends to use a 10-min or 30-min AEGL values if the release has a short period of time and the concentration graphs presents a short exposure duration for all points in the threat zone.

Table 4-1: Probit Parameters (TNO, 2005)

Chemical compound	n	a	b
Hydrogen Sulfide	1.9	-11.5	1

The threat zone for Amine Absorption Unit Scenario is presented in . The Amine Absorption Unit is located in node 3 in . The release duration for this scenario was 1 minute (the total inventory of the vessel is released before the blocking system action), so the AEGLs values for 10 minutes were used Table 4-2.

Table 4-2: Maximum distance reached for AEGLs for Amine Unit Scenario

AEGL	Distance
76 ppm = AEGL-3 [10 min]	689 m
41 ppm = AEGL-2 [10 min]	897 m
0.75 ppm = AEGL-1 [10 min]	4.0 km

Figure 4-1: Results from Amine Absorption Unit scenario

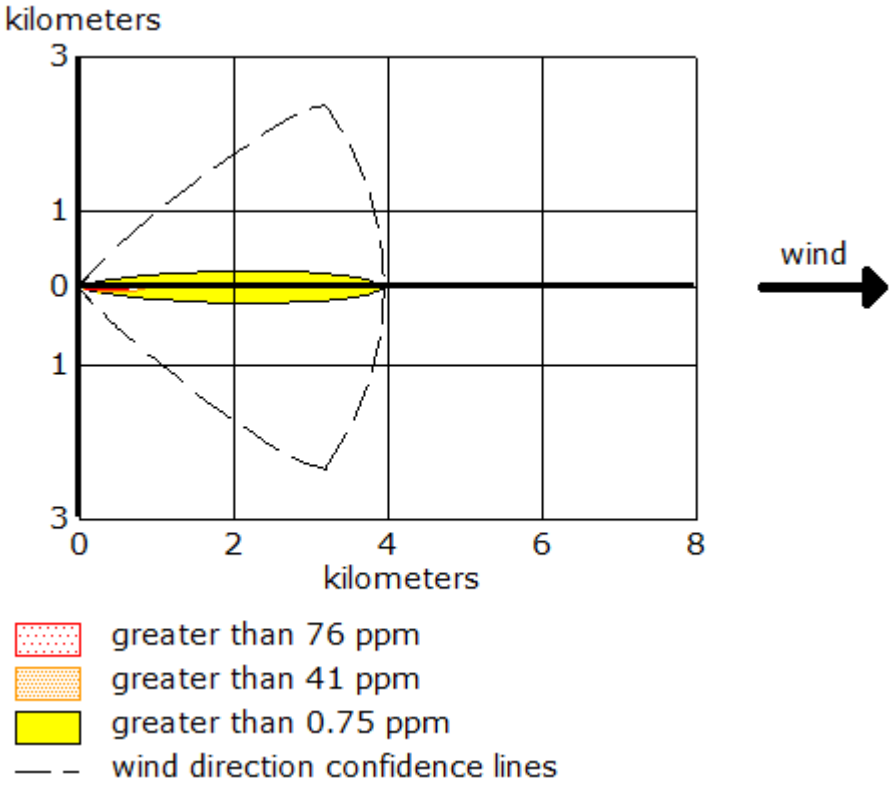

The threat zone for Sour Water Treatment Unit Scenario, located in node 4 in , is presented in . The release duration for this scenario was 1 minute (the total inventory of the vessel is released before the blocking system action), so the AEGLs values for 10 minutes were used (Table 4-3).

Table 4-3: Maximum distance reached for AEGLs for Sour Water Unit Scenario

AEGL	**Maximum Distance**
76 ppm = AEGL-3 [10 min]	1.2 km
41 ppm = AEGL-2 [10 min]	1.5 km
0.75 ppm = AEGL-1 [10 min]	6.3 km

Figure 4-2: Results from Sour Water Unit scenario

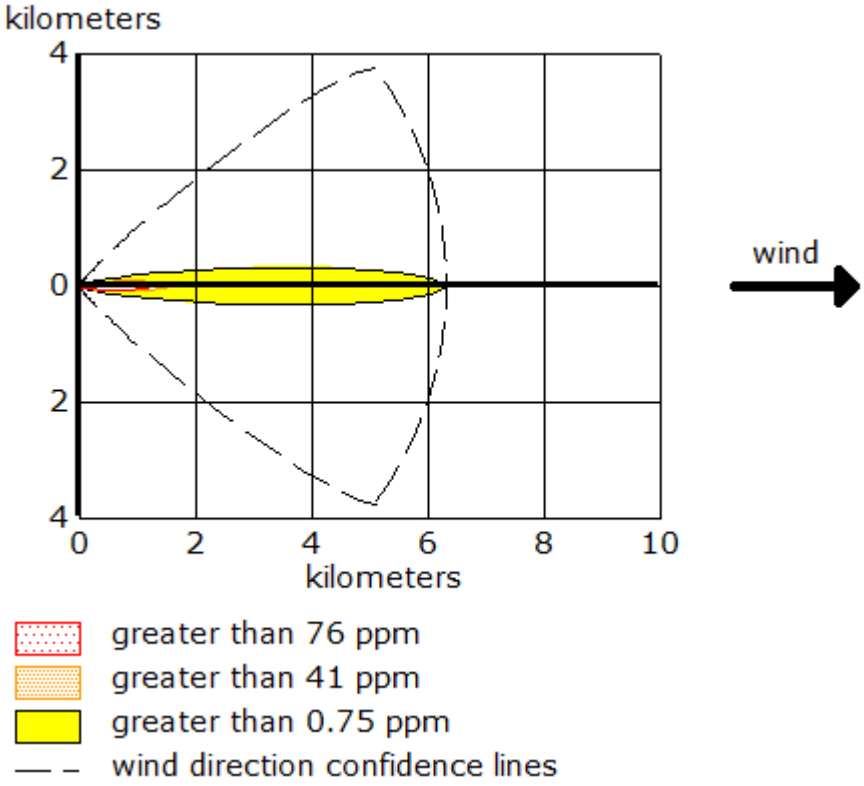

The threat zone for WSA Scenario, located in node 5 in , is presented in . The release duration for this scenario was 1 minute (the total inventory of the vessel is released before the blocking system action), so the AEGLs values for 10 minutes were used (Table 4-4).

Table 4-4: Maximum distance reached for AEGLs for WSA Scenario

AEGL	**Maximum Distance**
76 ppm = AEGL-3 [10 min]	134 meters
41 ppm = AEGL-2 [10 min]	186 meters
0.75 ppm = AEGL-1 [10 min]	1.2 kilometers

Figure 4-3: Results from WSA scenario

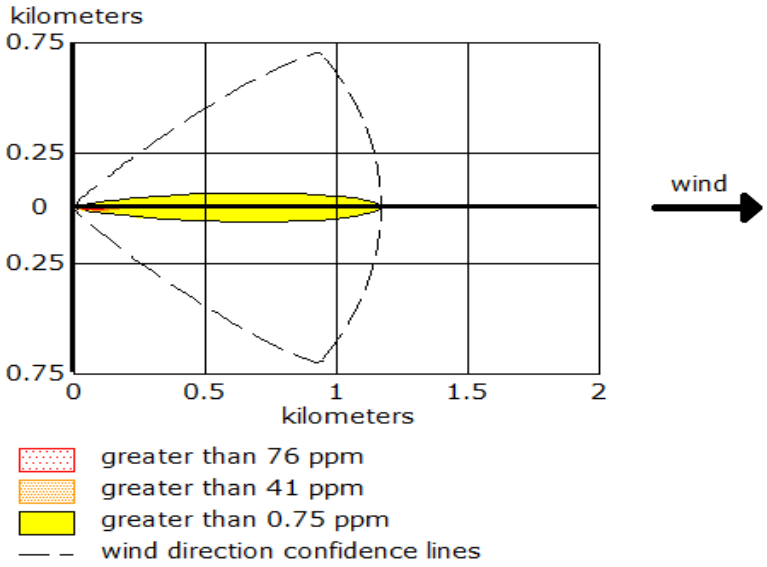

The maximum concentration achieved during the simulation was used to calculate the individual risk, one of the objective functions. The values for Amine Absorption Unit are presented in Table 4-5. The node where the unit is located (node 3) has the higher concentration value. The wind direction is from West South-West, therefore only the nodes located in this direction from the source presented a significant concentration value.

Table 4-5: Maximum concentration in nodes for Amine Absorption Unit scenario

Node	**Concentration (mg/m^3)**	**Node**	**Concentration (mg/m^3)**
1	0	11	0
2	0	12	0
3	436681	13	36.9111
4	0	14	40.3135
5	0	15	0
6	0	16	0
7	0	17	25.0723
8	242.662	18	21.3227
9	0	19	0
10	73.5457	20	0

The values for Sour Water unit are presented in Table 4-6. The node where the unit is located (node 4) has the higher concentration value. The wind direction is from West South-West, therefore only the nodes located in this direction from the source presented a significant concentration value. The node 20, considered as a safe zone, presented a significant concentration of 11mg/m³. However, this concentration corresponds to only 0.0144ppm, and it is not a risk to individuals (the AEGL-1 corresponds to a concentration higher than 0.75ppm).

Table 4-6: Maximum concentration in nodes for Sour Water scenario (node 4)

Node	**Concentration (mg/m³)**	**Node**	**Concentration (mg/m³)**
1	0	11	685.19
2	0	12	253.338
3	0	13	0
4	426408	14	194.518
5	7688.32	15	239.92
6	0	16	145.525
7	0	17	116.302
8	0	18	97.8302
9	0	19	130.485
10	0	20	47.2227

The values for WSA unit are presented in Table 4-7. The node where the unit is located (node 5) has the higher concentration value. The wind direction is from West South-West, therefore only the nodes located in this direction from the source presented a significant concentration value.

Table 4-7: Maximum concentration in nodes for WSA scenario

Node	Concentration (mg/m^3)	Node	Concentration (mg/m^3)
1	0	11	12.4619
2	0	12	0
3	0	13	0
4	0	14	0
5	528471	15	3.48388
6	0	16	1.95974
7	0	17	1.52205
8	0	18	1.2527
9	0	19	0
10	0	20	0

4.2 MOGA Results

The results obtained in this section considered the graph presented in . The refinery scenario simulated corresponds to all possible hazard events presented in section 3.2. The data about the evacuation escaping network (adjacency list and information about distance, initial velocity and the parameters α and β for each arc), the higher concentration in each node achieved during the entire simulation in ALOHA® (Table 4-5, Table 4-6 and Table 4-7) and the frequency of occurrence of a toxic cloud after a pipe rupture for each scenario were the input data of the MOGA algorithm.

The initial velocity considered was 110m/min (~1.83m/s) for each node and the minimum velocity an individual can achieve is 6m/min, considering the range presented in Shi et al. (2009). The parameters α and β were randomly generated and they have different ranges for each area, depending of the distance from the accidental event. The range applied were $\alpha \in [0,8;0,9]$ and $\beta \in [0,05;0,1]$ for area 1; $\alpha \in [0,9;0,9999]$ and $\beta \in [0,001;0,05]$ for area 2 and for the last area $\alpha \in [0,9999;0,99999]$ and $\beta \in [0,0001;0,001]$ (DE LIMA E SILVA, 2017). The range selected is related to the extension of the disaster, in the case of study it was selected a disaster grade 3 (YUAN; WANG, 2009). The higher the extension the disaster, the lower the value of α and lower the value of β.

The frequency for each accidental scenario were calculated using the event trees (Appendix 2) presented in Cetesb (2014). All the loss of containment frequencies used corresponds to a pipe rupture. The nominal diameter for every scenario are greater than 150mm, and then the frequency applied was $1 \times 10^{-7} m^{-1} y^{-1}$ (TNO, 2005). After that, using the event trees, the occurrence frequency per year of a toxic cloud dispersion after a pipe rupture was calculated (Table 4-8).

Table 4-8: Loss of containment frequency for the refinery accidental scenarios

Unit	**Pipe Length (m)**	**Loss of Containment Frequency (year^{-1})**	**Occurrence frequency in a year**
Amine Absorption	40	4.00×10^{-6}	1.80×10^{-6}
Sour Water Treatment	150	1.5×10^{-5}	6.75×10^{-6}
WSA	60	6.0×10^{-6}	2.70×10^{-6}

The MOGA algorithm considers the sum of the occurrence frequency of a toxic cloud scenario and the probability of death in each scenario simulated to calculate the individual risk for each route as presented in equation (2.1) and (2.2).

4.2.1 Model Validation

The proposed multi-objective genetic algorithm was validated by comparing the Pareto front obtained from the heuristic method and the exact one obtained from the exhaustive method. In the exhaustive method, all the possible solutions (routes) between the source and destination node were founded using an algorithm based on Depth First Search (DFS). The algorithm starts the search from the source and keeps storing the visited vertices in an array. If the destination node is reached, the contents of the array are printed. It is important to mark the current vertices in the array as visited, so that the search does not make cycles. After that, the objective functions were calculated for each possible solution and the non-dominated ones were selected among them. The parameters used in the MOGA are presented in Table 4-9.

Table 4-9: MOGA parameters

Parameters	Value
Population size	100
Number of generations	200
Probability of crossover	0.95
Probability of mutation	0.01

The point-to-point distance metric (LINS; DROGUETT, 2011) was applied to validate the MOGA model. The metric calculates the minimum Euclidean distance between each point obtained from MOGA and one of the points from the real front. All minimum distances *d*, , are summed up and divided by ns_k for each *k*th simulated front. After that, the weighted mean metric, *D*, is calculated by Equation (3.1). The metric tries to summarize the convergence of each simulated Pareto front in one single number.

$$D = \frac{\sum_k \bar{d}_k \times ns_k}{\sum_k ns_k} \ , k = 1, \dots, nsFronts \tag{4.1}$$

Figure 4-4: Point-to-point distance

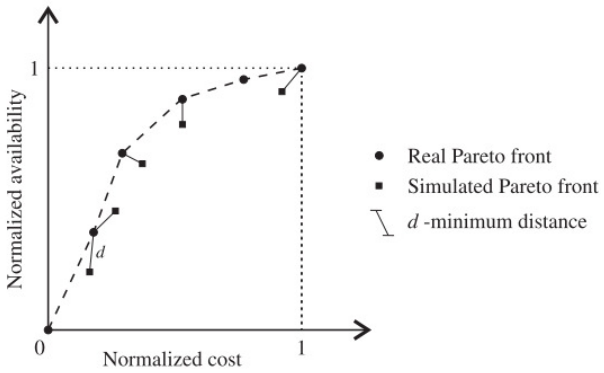

Source: (LINS; DROGUETT, 2011)

30 trials of MOGA were executed to calculate the distance metric and generate the descriptive statistics (minimum, maximum, mean and standard deviation) related to the number of solutions of each simulated Pareto Front and the number of exact Pareto solutions obtained (Table 4-10). The results show that in most of the simulations, MOGA founds approximately 10 of the 12 real solutions of the problem.

Table 4-10: Metrics and descriptive statics from the simulated Pareto Fronts

Distance Metrics	D	5.31E-03
Number of solutions	Min.	10
	Max.	16
	Mean	12.07
	Std.Dev	0.83
Exact solutions	Min.	6
	Max.	12
	Mean	9.53
	Std.Dev	1.55

Table 4-11 shows the mean and variance of minimum distances (var_k) for 30 obtained Pareto fronts. The solutions number 4, 6, 9, 13, and 23 were the best solutions and the solution number 17 was the worst solution found by MOGA.

Table 4-11: Mean and variance of minimum distances for 30 obtained Pareto fronts

k	$\bar{d}_k$	var_k	ns_k	k	$\bar{d}_k$	var_k	ns_k
1	6.65E-03	2.21E-04	12	16	6.65E-03	2.21E-04	12
2	6.65E-03	2.21E-04	12	17	7.98E-03	2.55E-04	10
3	6.65E-03	2.21E-04	12	18	6.65E-03	2.21E-04	12
4	5.07E-44	2.83E-86	12	19	6.65E-03	2.21E-04	12
5	6.65E-03	2.21E-04	12	20	6.65E-03	2.21E-04	12
6	5.07E-44	2.83E-86	12	21	6.65E-03	2.21E-04	12
7	6.66E-03	2.21E-04	12	22	6.65E-03	2.21E-04	12
8	6.65E-03	2.21E-04	12	23	5.07E-44	2.83E-86	12
9	5.07E-44	2.83E-86	12	24	6.65E-03	2.21E-04	12
10	6.65E-03	2.21E-04	12	25	6.65E-03	2.21E-04	12
11	6.65E-03	2.21E-04	12	26	6.65E-03	2.21E-04	12
12	1.80E-09	2.02E-17	12	27	6.65E-03	2.21E-04	12
13	5.07E-44	2.83E-86	12	28	5.41E-03	1.71E-04	16
14	6.65E-03	2.21E-04	12	29	6.65E-03	2.21E-04	12
15	6.65E-03	2.21E-04	12	30	6.65E-03	2.21E-04	12

The MOGA proposed is able to find the solutions and all of them are near the real Pareto front.

4.2.2 Model results for the evacuation route planning

In this section, the results for the evacuation route planning problem are discussed. The network presented in is divided in different areas that corresponds to different range of values

of the parameters α and β in equation (3.9) that calculates the individual speed. For cases 1 to 3 (Figure 4-5), the Area 1 is closer to the accidental scenarios so the parameters α and β have a high influence in the speed. The Area 2 and Area 3 has a minor impact in the evacuee velocity, because it is far away from the disaster. The values for α and β used are in Appendix 3.

Figure 4-5: Emergency evacuation route network, showing the three different areas for cases 1, 2 and 3

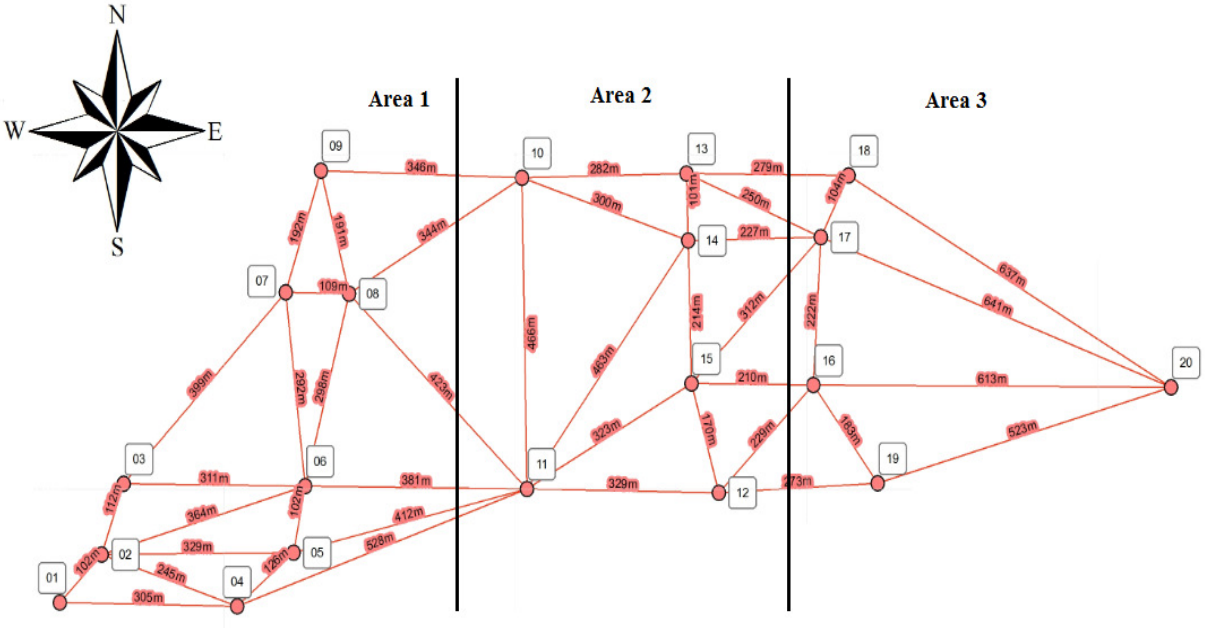

Adapted from (DE LIMA E SILVA, 2017).

Considering the start point as the node 1 (Case 1), the MOGA obtained a Pareto front of 12 possible solutions that must be analyzed by a decision maker, Table 4-12.

Table 4-12: Results from the evacuation problem proposed when the start point is node 1 (Case 1)

N	Route	Distance (m)	Evacuation Time (min)	Individual Risk
1	1-2-3-7-8-10-14-17-18-20	2334	31.118	1.8000030E-06
2	1-2-3-7-8-10-14-17-20	2234	30.206	1.8000039E-06
3	1-2-5-11-14-17-18-20	2274	29.922	9.4186466E-06
4	1-2-5-11-14-17-20	2174	29.010	9.4186495E-06
5	1-2-5-11-15-16-20	1989	28.770	9.4187031E-06
6	1-2-6-7-9-10-14-17-18-20	2564	88.436	9.1200143E-12
7	1-2-6-7-9-10-14-17-20	2464	87.523	1.1509924E-11
8	1-2-6-8-10-14-17-18-20	2376	38.230	2.6470766E-10
9	1-2-6-8-10-14-17-20	2276	37.318	2.6656353E-10
10	1-2-6-11-14-17-18-20	2278	35.523	1.2985109E-07
11	1-2-6-11-14-17-20	2178	34.611	1.3091352E-07
12	1-4-5-11-15-16-20	1989	27.838	9.4500000E-06

We can divide the routes 1, 2, 3, 4, 5 and 12 in set S_1 and routes 6, 7, 8, 9, 10 and 11 in set S_2. S_1 are the routes in the ALARP zone ($1 \times 10^{-6} year^{-1} \leq RI \leq 1 \times 10^{-5}$), and thus they only can be considered if the risk is reduced. S_2 are in the acceptable area, i.e., it means $RI < 1 \times 10^{-6} year^{-1}$. The decision maker can consider the following strategy to evacuation planning when the exact location of the accident is not available:

- The routes from S_2 must be consider with high priority for evacuees in node 1. The route 11 (1-2-6-11-14-17-20) is the best solution for the total travel time and an acceptable individual risk.
- The routes from S_1 only can be considered if the routes from S_2 are not available, for instance some of the paths from S_2 are blocked because of the accidental scenario. However, the evacuees must be wearing a protective device to use these routes. The route 2 (1-2-3-7-8-10-14-17-20) is the best route in respect to individual risk, because it is closer to the acceptable zone. Furthermore, the total time is lower than the total time from route 11.

The route 12 has the best total time, however the individual risk is the highest and it is very close to the upper limit between the ALARP and the non-acceptable zone. The route 12 shows the importance of considering the hazard to people in an evacuation planning, since the best evacuation time is not secure to people.

The Table 4-13 presents the routes if the evacuee starts at node 6 (Case 2). All the routes are in the acceptable zone so the route with the best evacuation time, route 1 (6-11-15-16-20) is the best option.

Table 4-13: Results from the evacuation problem starting point in node 6 (Case 2)

N	Route	Distance (m)	Evacuation Time (min)	Individual Risk
1	6-11-15-16-20	1527	17.292	4.163E-08
2	6-11-15-16-19-20	1620	18.141	4.157E-08
3	6-7-9-10-14-17-20	1998	25.006	3.595E-12
4	6-8-10-13-17-18-20	1915	23.831	1.271E-11
5	6-7-9-10-13-18-20	2028	31.482	6.134E-15
6	6-7-9-10-14-17-18-20	2098	25.917	2.694E-12
7	6-8-10-14-17-20	1810	20.301	1.434E-11
8	6-8-10-13-17-20	1815	22.920	1.282E-11
9	6-7-9-10-13-17-20	2003	29.251	4.423E-14
10	6-8-10-14-17-18-20	1910	21.212	1.342E-11
11	6-7-9-10-13-17-18-20	2103	30.163	2.031E-14

The comparison between the results of Table 4-12 and Table 4-13 shows the influence of the α and β parameters in the individual velocity, equation (3.9). As the starting point is the node 6, the individual takes less time in Area 1 (Figure 4-5). This area impacts the most in the evacuee velocity. For example, the route 6 of both cases are very similar but the total time is much higher in case 1, because the arc 1-2 and 2-6 belongs to the route and they are very close to the accidental scenario (Area 1).

In the case 3, the Amine Absorber Unit is in a different node, node 2. The concentration value is on Table 4-14. Table 4-15 shows the impact of changing a location of a possible accident. An evacuee, that starts in node 1, have to pass through one of the units to escape, so for all the routes, the individual risk is in the ALARP zone.

Table 4-14: Maximum concentration in nodes for Amine Absorber scenario (node 11)

Node	Concentration (mg/m^3)	Node	Concentration (mg/m^3)
1	0	11	0
2	0	12	0
3	436681	13	36.9111
4	0	14	40.3135
5	0	15	0
6	0	16	0
7	0	17	25.0723
8	242.662	18	21.3227
9	0	19	0
10	73.5457	20	0

Table 4-15: Results from the evacuation problem starting point in node 1 and Amine Absorber Unit in node 2 (Case 3)

N	Route	Distance (m)	Evacuation Time (min)	Individual Risk
1	1-2-3-7-8-10-13-17-20	2239	36.77	1.80E-06
2	1-2-3-7-8-10-13-18-20	2264	40.34	1.80E-06
3	1-4-5-11-15-16-20	1989	27.84	9.45E-6
4	1-2-3-7-8-10-13-17-18-20	2484	37.68	1.80E-06
5	1-2-3-7-8-10-14-17-20	2234	30.21	1.80E-06
6	1-4-5-11-14-17-20	2174	28.21	9.45E-6
7	1-2-3-7-8-10-14-17-18-20	2334	31.12	1.80E-06

In the case 4, only the Sour Water Unit is in a different node, node 11 (the maximum concentrations for this scenario are in Table 4-16). For this case, the Area 1 (Figure 4-5) expands to Area 2, it means, now Area 1 is equal to Area 1 and Area 2 together and the parameters α and β were changed (Appendix 3). The Table 4-17 shows that, although most of the solutions are in the acceptable zone for the individual risk, the evacuation time increased significantly. Such higher evacuation time could not be acceptable for the security of the evacuees.

Table 4-16: Maximum concentration in nodes for Sour Water Unit scenario (node 11)

Node	Concentration (mg/m^3)	Node	Concentration (mg/m^3)
1	0	11	12.5
2	0	12	0
3	0	13	0
4	0	14	0
5	528000	15	3.48388
6	0	16	1.95974
7	0	17	1.52205
8	0	18	1.2527
9	0	19	0
10	0	20	0

Table 4-17: Results from the evacuation problem starting point in node 1 and Sour Water Unit in node 11 (Case 4)

N	Route	Distance (m)	Evacuation Time (min)	Individual Risk
1	1-2-6-7-8-10-13-17-20	2384	128.90	1.96E-08
2	1-4-11-12-16-20	2004	78.14	6.75E-06
3	1-2-6-7-8-10-13-17-18-20	2484	129.82	4.17E-09
4	1-2-3-7-8-10-14-17-18-20	2334	84.28	1.80E-06
5	1-2-6-7-8-10-14-17-20	2379	128.07	1.98E-08
6	1-4-5-11-12-19-20	1968	55.10	9.45E-06
7	1-2-6-7-9-10-14-17-18-20	2564	140.98	3.49E-11
8	1-2-3-7-8-10-13-18-20	2264	90.27	1.80E-06
9	1-2-6-7-8-10-14-17-18-20	2449	128.98	4.38E-09
10	1-2-3-7-8-10-14-17-20	2334	83.37	1.81E-06
11	1-2-6-7-9-10-13-17-18-20	2396	141.82	2.89E-11
12	1-2-6-7-9-10-13-18-20	2494	145.66	2.04E-11

Case 3 and case 4 shows the importance of an analysis of the process units location during the project of a new refinery. The algorithm presented in this work can be used during this stage and give information for the decision maker to create an installation more secure.

5 CONCLUDING REMARKS

This work presented a Multi-Objective Genetic Algorithm to find the Pareto front of an evacuation planning problem that aims to minimize both the travel time and the individual risk a person is exposed along an evacuation route. This work also highlighted the risks in an oil refinery, concerning about an accidental hydrogen sulfide release in any of the treatment units: Amine Absorption Unit, Sour Water Treatment Unit and WSA Unit, which are responsible for removing H_2S from the products.

The accidental scenarios with higher severity were selected from the PHA. All the scenarios were simulated in ALOHA® software and their consequences were represented by a toxic threat zone that shows the area where the concentration is predicted to exceed the Level of Concern (LOC) after a time the release begins. The value of concentrations obtained are used to calculate the probability of death of an individual in the area, using the Probit function. After that, the frequency of a failure is calculated and finally the probability of death due to a toxic release is predicted. These data were input to the MOGA that calculates the non-dominated solutions. The comparison between MOGA results against the exhaustive method indicated that the Pareto fronts found by the heuristic model are very close to the real Pareto fronts. Thus, the MOGA could find exactly most of the solutions and for problems with a huge solution set, its application could be crucial. In addition, MOGA can find many the Pareto front in a single run, while in the modified Dijkstra algorithm presented by Gai et al. (2017) it is necessary to perform several runs to find the weight vector.

In total four different cases were presented. Two of them considered that any accidental scenario presented in 3.2 could happen and the evacuee starts at a different node. The node 1 is one the worse starting points to an evacuee, because the individual is closer to any of the possible accidental scenarios. Case 3 and 4 tried to emphasize the importance of a detailed study during the project of a chemical installation, important decisions at the stage could badly impact the security of an installation.

5.1 Limitations and suggestions for future works

All the consequences calculation in ALOHA® consider that all the streams compositions were 100% hydrogen sulfide, as the software could not simulate chemical mixtures. Because of that, in this work, all the scenarios considered have the highest concentration of hydrogen sulfide (more than 70% of mass fraction) in order to be more realistic. It could be interesting to use another software that considers chemical mixtures, because there are another important scenarios in an oil refinery with a significant amount of hydrogen sulfide although the mass fraction is low (streams with high inventory).

MOGA is a probabilistic model and does not guarantee that the real optimal solutions will be achieved. Nevertheless, this handicap can be minimized if multiple runs are performed with different GA parameters (size of the population, number of generations, crossover and mutation probability).

Future works may consider many other accidental scenarios from a refinery to be closer to the reality. Also, the escaping route network can be redone to increase their number of nodes and arcs and give more detailed information about the best escaping routes. Some other ways of escaping can be considered such as use of vehicles and an inclusion of others objective functions like societal risk. Furthermore, for an evacuation route planning it is important to consider also the capacity of the network, applying a maximum flow problem algorithm.

REFERENCES

ALE, B. J. M.; KLUIN, M. H. A.; KOOPMANS, I. M. Safety in the Dutch chemical industry 40 years after Seveso. **Journal of Loss Prevention in the Process Industries**, v. 47, p. 203–209, 2017. Retrieved from: <http://dx.doi.org/10.1016/j.jlp.2017.04.010>.

APOSTOLAKIS, G. E. Uncertainty in Probabilistic Safety Assessment. **Nuclear Engineering and Design**, v. 115, p. 173–179, 1989. Retrieved from: <http://ac.els-cdn.com/0029549389902689/1-s2.0-0029549389902689-main.pdf?_tid=476ec1f6-dda3-11e6-84cb-00000aab0f26&acdnat=1484760583_a68cf70c98935c3b6929cb84a1d6acd9>.

CETESB. **Acidentes ambientais na indústria química e no armazenamento**. Retrieved from: <http://emergenciasquimicas.cetesb.sp.gov.br/tipos-de-acidentes/industrias-de-armazenamentos/introducao-industrias-de-armazenamentos/>. Acesso em: 19 jan. 2017.

CETESB. Risco de Acidente de Origem Tecnológica – Método para decisão e termos de referências. **Norma Técnica P4.261**, v. 2 edição, n. 11, p. 1–140, 2014.

COELLO COELLO, C. A.; LAMONT, G. L.; VAN VELDHUIZEN, D. A. **Evolutionary algorithms for solving multi-objective problems**. 2nd. ed. Berlin, Heidelberg: Springer, 2007.

DE LIMA E SILVA, G. T. **Aplicação do algoritmo de dijkstra na otimização multiobjetivo de rotas de evacuação em cenários de nuvem tóxica**. 2017. 100p. (Master - Programa de pós-graduação em engenharia de produção/ UFPE)

DUARTE, M. **Riscos industriais: etapas para a investigação e a prevenção de acidentes**. Rio de Janeiro: FUNENSEG, 2002.

ECKHOFF, R. K. Boiling liquid expanding vapour explosions (BLEVEs): A brief review. **Journal of Loss Prevention in the Process Industries**, v. 32, n. 1, p. 30–43, 2014. Retrieved from: <http://dx.doi.org/10.1016/j.jlp.2014.06.008>.

FAHIM, M. A.; AL-SAHHAF, T. A.; ELKILANI, A. S. **Fundamentals of petroleum refining**. First ed. Oxford: Elsevier, 2010.

FAHIM, M. A.; AL-SAHHAF, T. A.; ELKILANI, A. S. **Introdução ao refino de petróleo**. Rio de Janeiro: Editora Elsevier, 2012.

FINGAS, M. Chapter 3 – Introduction to Oil Chemistry and Properties. In: FINGAS, M. (Ed.). **Oil Spill Science and Technology**. First ed. [s.l.] John Wiley & Sons, 2015. p. 51–59.

GAI, W.; DENG, Y.; JIANG, Z.; LI, J.; DU, Y. Multi-objective evacuation routing optimization for toxic cloud releases. **Reliability Engineering & System Safety**, v. 159, n. October 2016, p. 58–68, 2017. Retrieved from: <http://dx.doi.org/10.1016/j.ress.2016.10.021>.

GEORGIADOU, P. S.; PAPAZOGLOU, I. A.; KIRANOUDIS, C. T.; MARKATOS, N. C. Modeling emergency evacuation for major hazard industrial sites. **Reliability Engineering and System Safety**, v. 92, n. 10, p. 1388–1402, 2007.

GEORGIADOU, P. S.; PAPAZOGLOU, I. A.; KIRANOUDIS, C. T.; MARKATOS, N. C. Multi-objective evolutionary emergency response optimization for major accidents. **Journal of Hazardous Materials**, v. 178, n. 1–3, p. 792–803, 2010. Retrieved from:

<http://dx.doi.org/10.1016/j.jhazmat.2010.02.010>.

GOERIGK, M.; DEGHDAK, K.; HESSLE, P. A comprehensive evacuation planning model and genetic solution algorithm. **Transportation Research Part E: Logistics and Transportation Review**, v. 71, p. 82–97, 2014. Retrieved from: <http://dx.doi.org/10.1016/j.tre.2014.08.007>.

GUPTA, J. P. Bhopal and the Global Movement on Process Safety. **IChemE Symposium Series**, n. 150, p. 1–12, 2004.

IKEDA, Y.; INOUE, M. An Evacuation Route Planning for Safety Route Guidance System after Natural Disaster Using Multi-Objective Genetic Algorithm. **Procedia - Procedia Computer Science**, v. 96, p. 1323–1331, 2016. Retrieved from: <http://dx.doi.org/10.1016/j.procs.2016.08.177>.

JAMES G. SPEIGHT. **The chemistry and technology of petroleum**. Fifth Edit ed. [s.l.] CRC Press, 1982. v. 5

JONES, R., W. LEHR, D. SIMECEK-BEATTY, R. M. R. ALOHA (Areal Locations Of Hazardous Atmospheres): Technical Documentation. n. November, 2013.

JORNAL ESTADÃO DIGITAL. **Vazamento de produto químico atinge Santos e Guarujá**. Retrieved from: <http://sao-paulo.estadao.com.br/noticias/geral,vazamento-atinge-patio-de-cargas-no-guaruja,10000007092>. Acesso em: 17 jan. 2017.

KHAN, F.; RATHNAYAKA, S.; AHMED, S. Methods and models in process safety and risk management: Past, present and future. **Process Safety and Environmental Protection**, v. 98, p. 116–147, 2015. Retrieved from: <http://dx.doi.org/10.1016/j.psep.2015.07.005>.

KONAK, A.; COIT, D. W.; SMITH, A. E. Multi-objective optimization using genetic algorithms: A tutorial. **Reliability Engineering and System Safety**, v. 91, n. 9, p. 992–1007, 2006.

LAURSEN, J. K. Details advances in sulphur recovery by the WSA process-The process principles. **Hydrocarbon Engineering**, n. August, 2007.

LAURSEN, J. K.; KARAVANOV, A. N. Processes for sulfur recovery, regeneration of spent acid, and reduction of NO x emissions. **Chemical and Petroleum Engineering**, v. 42, n. 5–6, p. 229–234, 2006.

LI, Q.; FANG, Z.; LI, Q.; ZONG, X. Multiobjective Evacuation Route Assignment Model Based on Genetic Algorithm. **2010 18th International Conference on Geoinformatics**, p. 1–5, 2010. Retrieved from: <http://ieeexplore.ieee.org/lpdocs/epic03/wrapper.htm?arnumber=5567485>.

LINS, I. D. **Models for quantifying risk and reliability metrics via metaheuristics and support vector machines**. 2013. 112p. (PhD - Pograma de pós-graduação em engenharia de produção/ UFPE)

LINS, I. D.; DROGUETT, E. L. Redundancy allocation problems considering systems with imperfect repairs using multi-objective genetic algorithms and discrete event simulation. **Simulation Modelling Practice and Theory**, v. 19, n. 1, p. 362–381, 2011. Retrieved from: <http://dx.doi.org/10.1016/j.simpat.2010.07.010>.

MAHON, J. F.; KELLEY, P. C. Managing toxic wastes-After Bhopal and Sandoz. **Long Range Planning**, v. 20, n. 4, p. 50–59, 1987.

MARHAVILAS, P. K.; KOULOURIOTIS, D.; GEMENI, V. Risk analysis and assessment methodologies in the work sites: On a review, classification and comparative study of the scientific literature of the period 2000-2009. **Journal of Loss Prevention in the Process Industries**, v. 24, n. 5, p. 477–523, 2011. Retrieved from: <http://dx.doi.org/10.1016/j.jlp.2011.03.004>.

MELO, E. N. **O efeito da simulação de multidão na segurança e no estudo de layout**. 2015. 70p. (Master - Programa de pós-graduação em engenharia de produção/ UFPE)

MILAZZO, M. F.; AVEN, T. An extended risk assessment approach for chemical plants applied to a study related to pipe ruptures. **Reliability Engineering and System Safety**, v. 99, p. 183–192, 2012. Retrieved from: <http://dx.doi.org/10.1016/j.ress.2011.12.001>.

MORAES, G. **Sistema de gestão de riscos. estudos de análise de riscos "offshore e onshore"**. 1. ed. Rio de Janeiro: Livraria Virtual, 2013.

NATIONAL RESEARCH COUNCIL. **Acute exposure guideline levels for selected airborne chemicals**. [s.l.] The National Academies Press, 2010. v. 9

NOAA. **Acute Exposure Guideline Levels (AEGLs)**. Retrieved from: <https://response.restoration.noaa.gov/oil-and-chemical-spills/chemical-spills/resources/acute-exposure-guideline-levels-aegls.html>. Acesso em: 6 nov. 2017a.

NOAA. **Ask Dr. ALOHA: Choosing Toxic Levels of Concern**. Retrieved from: <https://response.restoration.noaa.gov/ADA/toxiclocs>. Acesso em: 6 nov. 2017b.

NOAA. **Toxic Levels of Concern**. Disponível em: <https://response.restoration.noaa.gov/oil-and-chemical-spills/chemical-spills/resources/toxic-levels-concern.html>. Acesso em: 6 nov. 2017c.

OLIVEIRA, L. F. **Incêndio na Vale Fertilizantes gera grande nuvem de fumaça tóxica em Cubatão**. Retrieved from: <http://www.abrisco.com.br/novo/noticias-de-interesse/noticias-sobre-acidentes/item/63-incendio-na-vale-fertilizantes>. Acesso em: 31 out. 2017.

RAUSAND, M. **Risk assessment: theory, methods, and applications**. [s.l.] John Wiley & Sons, 2006.

SAADATSERESHT, M.; MANSOURIAN, A.; TALEAI, M. Evacuation planning using multiobjective evolutionary optimization approach. **European Journal of Operational Research**, v. 198, n. 1, p. 305–314, 2009. Retrieved from: <http://dx.doi.org/10.1016/j.ejor.2008.07.032>.

SANTOS, Y. A. C. **Seleção de rotas de evacuação utilizando métodos de otimização**. 2016. (Undergraduate thesis - Departamento de engenharia de produção/ UFPE)

SHEN, Y.; WANG, Q.; YAN, W.; SUN, J. An evacuation model coupling with toxic effect for chemical industrial park. **Journal of Loss Prevention in the Process Industries**, v. 33, p. 258–265, 2015. Retrieved from: <http://dx.doi.org/10.1016/j.jlp.2015.01.002>.

SHI, L.; XIE, Q.; CHENG, X.; CHEN, L.; ZHOU, Y.; ZHANG, R. Developing a database for emergency evacuation model. **Building and Environment**, v. 44, n. 8, p. 1724–1729, 2009.

Retrieved from: <http://dx.doi.org/10.1016/j.buildenv.2008.11.008>.

SORENSEN, J. H.; SHUMPERT, B. L.; VOGT, B. M. Planning for protective action decision making: Evacuate or shelter-in-place. **Journal of Hazardous Materials**, v. 109, n. 1–3, p. 1–11, 2004.

TNO - NETHERLANDS ORGANISATION FOR APPLIED SCIENTIFIC RESEARCH. **Red book - methods for determining and processing probabilities**. 4. ed. [s.l.] Gevaarlijke Stoffen, 2005a. v. 4

TNO - NETHERLANDS ORGANISATION FOR APPLIED SCIENTIFIC RESEARCH. **Purple book - guidelines for quantitative risk assessment**. 3. ed. [s.l.] Gevaarlijke Stoffen, 2005b.

VALE. **Esclarecimento sobre incêndio em Cubatão**. Retrieved from: <http://www.valefertilizantes.com/valefertilizantes/noticiaDetalhada.asp?noticia_id=416&utm_source=google&utm_medium=cpc&utm_term=%2Bvale %2Bcubatão&utm_campaign=vale_fertilizantes_cubatao&gclid=CNqt0qnOttECFQcGkQodly8EsQ>. Acesso em: 31 oct. 2017.

VILLA, V.; PALTRINIERI, N.; KHAN, F.; COZZANI, V. Towards dynamic risk analysis: A review of the risk assessment approach and its limitations in the chemical process industry. **Safety Science**, v. 89, p. 77–93, 2016. Retrieved from: <http://dx.doi.org/10.1016/j.ssci.2016.06.002>.

VUORIO, A.; STOOP, J.; JOHNSON, C. The need to establish consistent international safety investigation guidelines for the chemical industries. **Safety Science**, v. 95, p. 62–74, 2017. Disponível em: <http://dx.doi.org/10.1016/j.ssci.2017.02.003>.

XU, J.-H.; FAN, Y. An individual risk assessment framework for high-pressure natural gas wells with hydrogen sulphide, applied to a case study in China. **Safety Science**, v. 68, p. 14–23, out. 2014. Retrieved from: <http://linkinghub.elsevier.com/retrieve/pii/S0925753514000393>. Acesso em: 17 ago. 2017.

YUAN, Y.; WANG, D. Path selection model and algorithm for emergency logistics management. **Computers & Industrial Engineering**, v. 56, n. 3, p. 1081–1094, 2009. Disponível em: <http://www.sciencedirect.com/science/article/pii/S0360835208002234>.

ZHOU, Y.; LIU, M. Risk Assessment of Major Hazards and its Application in Urban Planning: A Case Study. **Risk Analysis**, v. 32, n. 3, p. 566–577, 2012.

ZHU, M.; SUN, L.; OU, G.; WANG, K.; WANG, K.; SUN, Y. Erosion corrosion failure analysis of the elbow in sour water stripper overhead condensing reflux system. **Engineering Failure Analysis**, v. 62, p. 93–102, 2016. Retrieved from: <http://dx.doi.org/10.1016/j.engfailanal.2016.01.002>.

APPENDIXES

Appendix 1

A risk assessment requires an analysis to identify the main hazards in a facility as described in subtopic 1.1. Preliminary risk analysis was the qualitative technique used in this work.

AMINE ABSORPTION UNIT

Facility: Oil Refinery				
Process Unity: Amine Absorption Unit				
System element description: Stripper knockout drum top outlet pipe				
Hazard	**Cause**	**Consequences**	**Severity Class**	**Prevention measures and Risk-reducing measures**
Rich amine (amine + H_2S)	Pipe rupture due to: ✓ Corrosion ✓ Incorrect operation ✓ Material failure of pipe or weld	Toxic Cloud	IV	• Ensure quality in construction and assembly; • Have a preventive maintenance program (including corrosion prevention and control program) • Workers must have a hydrogen sulfide portable gas detector

Facility: Oil Refinery				
Process Unity: Amine Absorption Unit				
System element description: Stripper knockout drum top outlet pipe				
Hazard	**Cause**	**Consequences**	**Severity Class**	**Prevention measures and Risk-reducing measures**
Acid Gas release (H_2S)	Pipe rupture due to: ✓ Corrosion ✓ Incorrect operation ✓ Material failure of pipe or weld	Toxic Cloud	IV	• Ensure quality in construction and assembly; • Have a preventive maintenance program (including corrosion prevention and control program) • Workers must have a hydrogen sulfide portable gas detector

SOUR WATER TREATMENT UNIT

Facility: Oil Refinery				
Process Unity: Sour Water Treatment Unit				
System element description: Sour water stripper top outlet pipe				
Hazard	**Cause**	**Consequences**	**Severity Class**	**Prevention measures and Risk-reducing measures**
Acid Gas release (H_2S)	Pipe rupture due to: ✓ Corrosion ✓ Incorrect operation ✓ Material failure of pipe or weld	Toxic Cloud	V	• Ensure quality in construction and assembly; • Have a preventive maintenance program (including corrosion prevention and control program) • Workers must have a hydrogen sulfide portable gas detector

WSA UNIT

Facility: Oil Refinery				
Process Unity: WSA Unit				
System element description: Feed knockout drum outlet pipe				
Hazard	**Cause**	**Consequences**	**Severity Class**	**Prevention measures and Risk-reducing measures**
Acid Gas release (H_2S)	Pipe rupture due to: ✓ Corrosion ✓ Incorrect operation ✓ Material failure of pipe or weld	Toxic Cloud	IV	• Ensure quality in construction and assembly; • Have a preventive maintenance program (including corrosion prevention and control program) • Workers must have a hydrogen sulfide portable gas detector

Appendix 2

The individual risk calculation requires the probability of failure. All scenarios simulated correspond to a pipe rupture, so the frequency was calculated using the data in the Purple Book (TNO, 2005). An event tree for a toxic and flammable gas release is presented below:

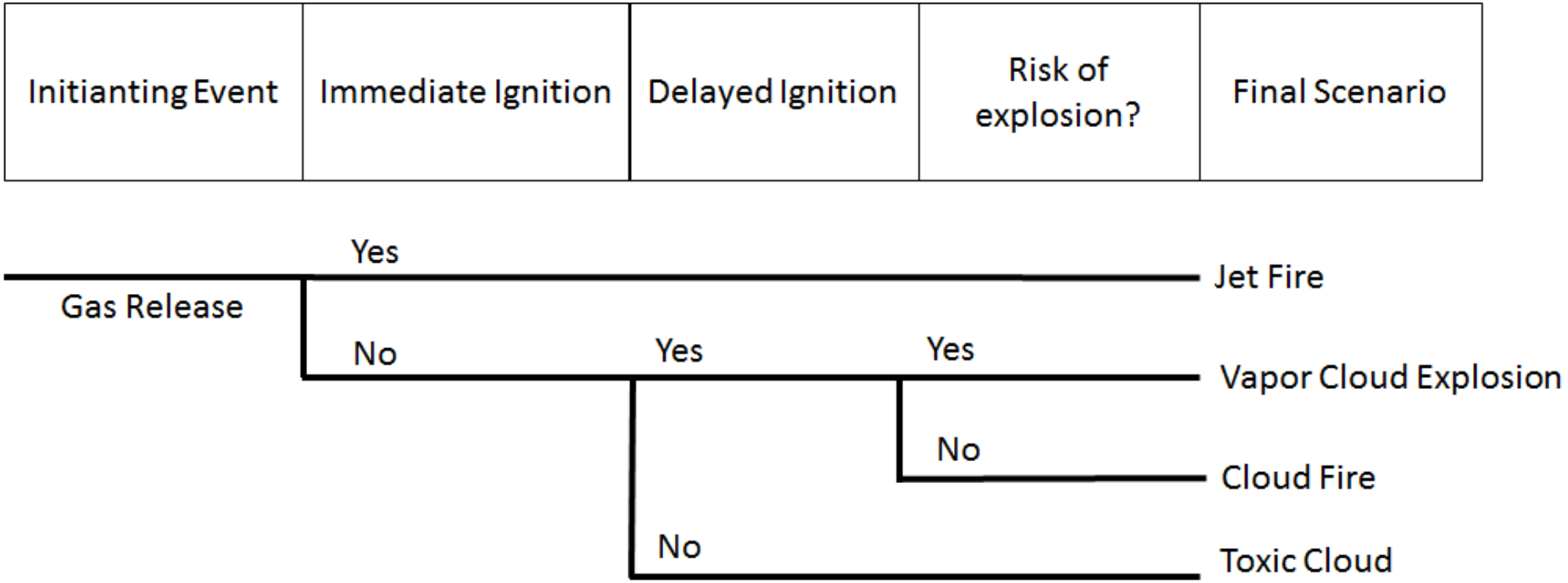

AMINE ABSORPTION UNIT

Initianting Event	Immediate Ignition	Delayed Ignition	Risk of explosion?	Final Scenario

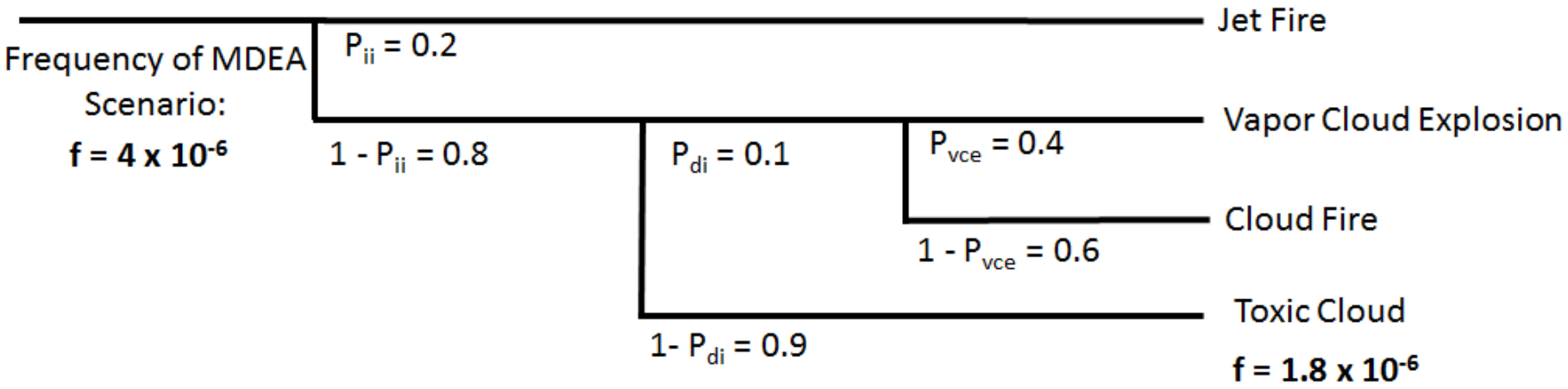

SOUR WATER TREATMENT

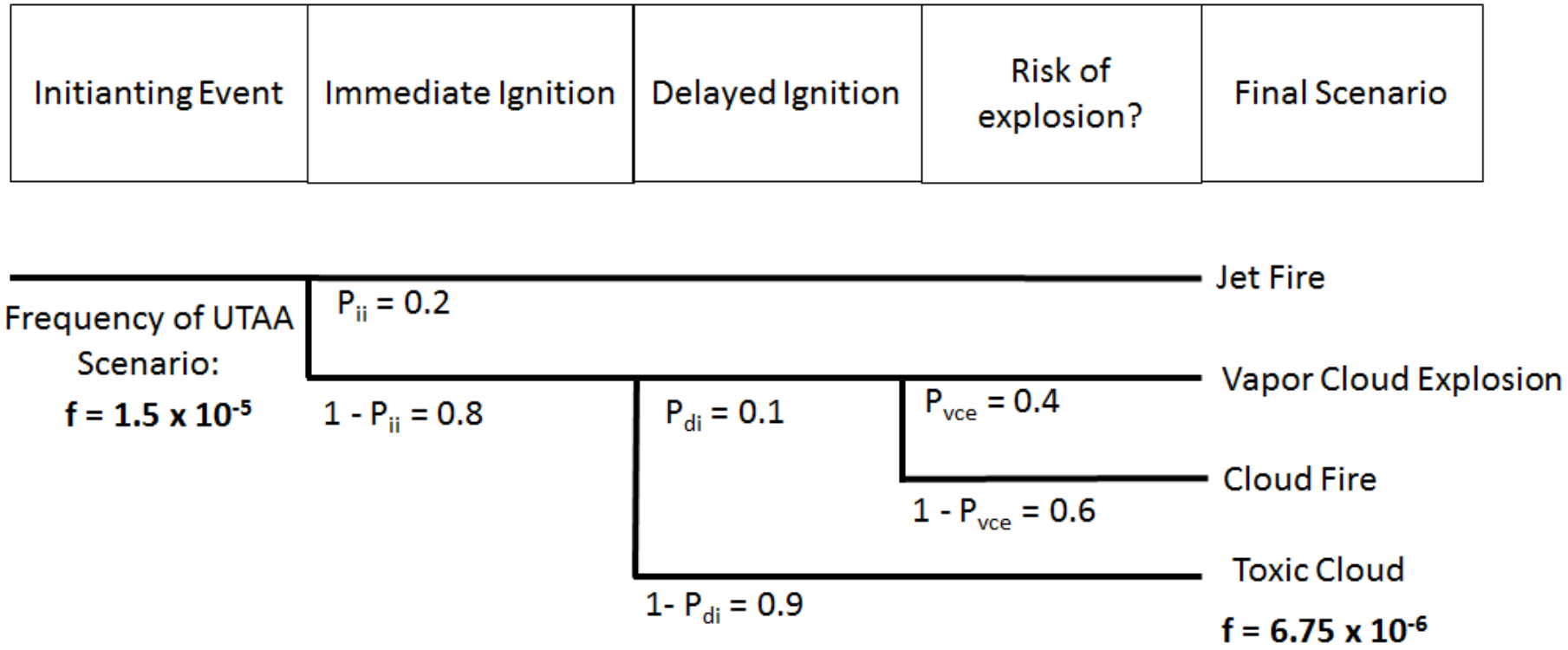

WSA

Initianting Event	Immediate Ignition	Delayed Ignition	Risk of explosion?	Final Scenario

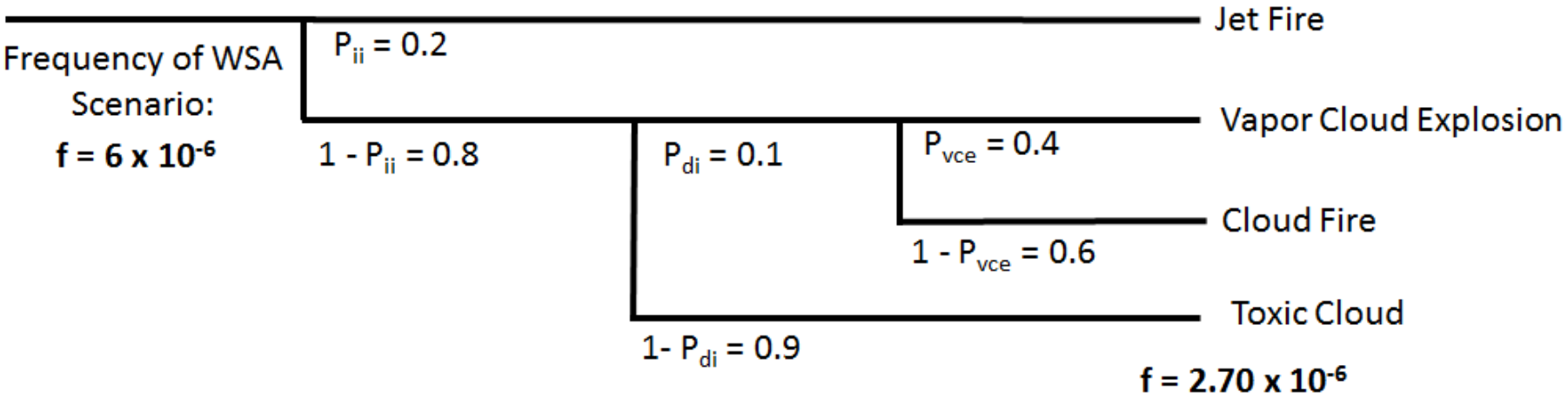

Appendix 3

Values of α and β for cases 1, 2 and 3.

i	j	α	β
1	2	0.833556	0.0886678
1	4	0.887563	0.0958481
2	4	0.857795	0.0878213
2	3	0.861845	0.0821438
2	5	0.888587	0.0941961
2	6	0.84875	0.0705588
3	6	0.81291	0.0737742
3	7	0.849565	0.059842
4	5	0.870846	0.0539262
4	11	0.837464	0.0887858
5	6	0.870846	0.0584944
5	11	0.839837	0.0616295
6	7	0.888494	0.0732234
6	8	0.81496	0.0908331
6	11	0.859618	0.0953738
7	8	0.872211	0.0657979
7	9	0.813565	0.0556658
8	9	0.884879	0.0633769
8	10	0.91889	0.0595884
8	11	0.9960979	0.0615875
9	10	0.974439	0.0854518
10	11	0.979239	0.0384873

i	j	α	β
10	13	0.901867	0.0383857
10	14	0.989872	0.0011587
11	12	0.963652	0.0484989
11	14	0.975876	0.0226442
11	15	0.934161	0.0435435
12	15	0.976196	0.0271564
12	16	0.974394	0.0327381
12	19	0.959553	0.0302423
13	14	0.929228	0.0316732
13	17	0.988547	0.0321225
13	18	0.925478	0.0409958
14	15	0.865616	0.0455336
14	17	0.829847	0.00599703
15	16	0.926732	0.0103853
15	17	0.967652	0.0367685
16	17	0.999939	0.000793486
16	19	0.999908	0.000188371
16	20	0.999939	0.000427569
17	18	0.999939	0.000427259
17	20	0.999969	0.000579442
18	20	0.999969	0.000518815
19	20	0.999908	0.000457778

Values of α and β for case 4.

i	j	α	β
1	2	0.833556	0.0886678
1	4	0.887563	0.0958481
2	4	0.857795	0.0878213
2	3	0.861845	0.0821438
2	5	0.888587	0.0941961
2	6	0.84875	0.0705588
3	6	0.81291	0.0737742
3	7	0.849565	0.059842
4	5	0.870846	0.0539262
4	11	0.837464	0.0887858
5	6	0.870846	0.0584944
5	11	0.839837	0.0616295
6	7	0.888494	0.0732234
6	8	0.81496	0.0908331
6	11	0.859618	0.0953738
7	8	0.872211	0.0657979
7	9	0.813565	0.0556658
8	9	0.884879	0.0633769
8	10	0.888494	0.0732234
8	11	0.872211	0.0657979
9	10	0.888494	0.0732234
10	11	0.839837	0.0616295

i	j	α	β
10	13	0.813565	0.0556658
10	14	0.813565	0.0556658
11	12	0.884879	0.0633769
11	14	0.81496	0.0908331
11	15	0.81496	0.0908331
12	15	0.872211	0.0657979
12	16	0.81496	0.0908331
12	19	0.839837	0.0616295
13	14	0.81496	0.0908331
13	17	0.861845	0.0821438
13	18	0.861845	0.0821438
14	15	0.865616	0.0455336
14	17	0.833556	0.0886678
15	16	0.833556	0.0886678
15	17	0.837464	0.0887858
16	17	0.999939	0.000793486
16	19	0.999908	0.000188371
16	20	0.999939	0.000427569
17	18	0.999939	0.000427259
17	20	0.999969	0.000579442
18	20	0.999969	0.000518815
19	20	0.999908	0.000457778